Materials Today Bio 23 (2023) 100829

Contents lists available at ScienceDirect

Materials Today Bio

journal homepage: www.journals.elsevier.com/materials-today-bio

Smart alginate inks for tissue engineering applications

Mozhgan Keshavarz [a,b], Mohammadjavad Jahanshahi [c], Masoud Hasany [d], Firoz Babu Kadumudi [e], Mehdi Mehrali [d], Mohammad-Ali Shahbazi [f,g], Parvin Alizadeh [a,*], Gorka Orive [b,h,i,j,**], Alireza Dolatshahi-Pirouz [e,***]

[a] Department of Materials Science and Engineering, Faculty of Engineering & Technology, Tarbiat Modares University, P. O. Box: 14115-143, Tehran, Iran
[b] NanoBioCel Research Group, School of Pharmacy, University of the Basque Country (UPV/EHU), Vitoria-Gasteiz 01006, Spain
[c] Department of Chemistry, Faculty of Science, University of Jiroft, P. O. Box 8767161167, Jiroft, Iran
[d] Department of Civil and Mechanical Engineering, Technical University of Denmark, 2800 Kgs. Lyngby, Denmark
[e] Department of Health Technology, Technical University of Denmark, 2800 Kgs. Lyngby, Denmark
[f] Department of Biomedical Engineering, University Medical Center Groningen, University of Groningen, Antonius Deusinglaan 1, 9713 AV, Groningen, the Netherlands
[g] W.J. Kolff Institute for Biomedical Engineering and Materials Science, University of Groningen, Antonius Deusinglaan 1, 9713 AV, Groningen, the Netherlands
[h] Biomedical Research Networking Centre in Bioengineering, Biomaterials and Nanomedicine (CIBER-BBN). Vitoria-Gasteiz 01006, Spain
[i] University Institute for Regenerative Medicine and Oral Implantology - UIRMI (UPV/EHU-Fundación Eduardo Anitua), Vitoria-Gasteiz 01006, Spain
[j] Bioaraba, NanoBioCel Research Group, Vitoria-Gasteiz 01006, Spain

ARTICLE INFO

Keywords:
Bioprinting
3D bioprinting
4D bioprinting
Tissue engineering
Hydrogels

ABSTRACT

Amazing achievements have been made in the field of tissue engineering during the past decades. However, we have not yet seen fully functional human heart, liver, brain, or kidney tissue emerge from the clinics. The promise of tissue engineering is thus still not fully unleashed. This is mainly related to the challenges associated with producing tissue constructs with similar complexity as native tissue. Bioprinting is an innovative technology that has been used to obliterate these obstacles. Nevertheless, natural organs are highly dynamic and can change shape over time; this is part of their functional repertoire inside the body. 3D-bioprinted tissue constructs should likewise adapt to their surrounding environment and not remain static. For this reason, the new trend in the field is 4D bioprinting – a new method that delivers printed constructs that can evolve their shape and function over time. A key lack of methodology for printing approaches is the scalability, easy-to-print, and intelligent inks. Alginate plays a vital role in driving innovative progress in 3D and 4D bioprinting due to its exceptional properties, scalability, and versatility. Alginate's ability to support 3D and 4D printing methods positions it as a key material for fueling advancements in bioprinting across various applications, from tissue engineering to regenerative medicine and beyond. Here, we review the current progress in designing scalable alginate (Alg) bioinks for 3D and 4D bioprinting in a "dry"/air state. Our focus is primarily on tissue engineering, however, these next-generation materials could be used in the emerging fields of soft robotics, bioelectronics, and cyborganics.

1. Introduction

Due to the rapidly aging population, age-related tissue and organ pathologies are rising. A possible avenue for addressing these problems is through tissue engineering; which is an alternative to organ transplantations. This concept is mainly based on biomaterial scaffolds that, via native-like biochemical and physical signals, can direct cells into desirable fates capable of facilitating tissue growth and regeneration [1–4]. Among the several commercially available scaffolds, hydrogels are considered very important for tissue engineering since they recapitulate many important aspects of the native cellular microenvironment [5]. In brief, hydrogels are made from crosslinked polymeric networks that can retain and absorb large amounts of water and, therefore, provide a wet 3D microenvironment that enables efficient

* Corresponding author. Department of Materials Science and Engineering, Faculty of Engineering & Technology, Tarbiat Modares University, P. O. Box: 14115-143, Tehran, Iran.
** Corresponding author. NanoBioCel Research Group, School of Pharmacy, University of the Basque Country (UPV/EHU), Vitoria-Gasteiz 01006, Spain.
*** Corresponding author. Department of Health Technology, Technical University of Denmark, 2800 Kgs. Lyngby, Denmark.
E-mail addresses: P-Alizadeh@modares.ac.ir (P. Alizadeh), gorka.orive@ehu.es (G. Orive), aldo@dtu.dk (A. Dolatshahi-Pirouz).

https://doi.org/10.1016/j.mtbio.2023.100829
Received 26 June 2023; Received in revised form 4 September 2023; Accepted 2 October 2023
Available online 4 October 2023

waste and nutrient exchange to support proper cell function [6,7]. The main drawbacks of these methods arise from the uneven dispersion of viable cells, occurring when cells are not thoroughly mixed during the hydrogel formulation but are instead seeded onto pre-formed hydrogel scaffolds and the challenges associated with the accurate positioning of different cell and material types to fully recapitulate the architectural complexities of native tissues.

3D multi-extrusion printing can address the abovementioned limitations by simultaneously using many nozzles [8–11] to deposit different cell and material types at pre-determined locations. However, they exhibit some limitations such, as limited material selection, slow printing speeds, and challenges with achieving multi-layer prints. Indeed; printing multiple layers is typically haunted by low fidelity and possible spillover of materials and cells into adjacent areas.

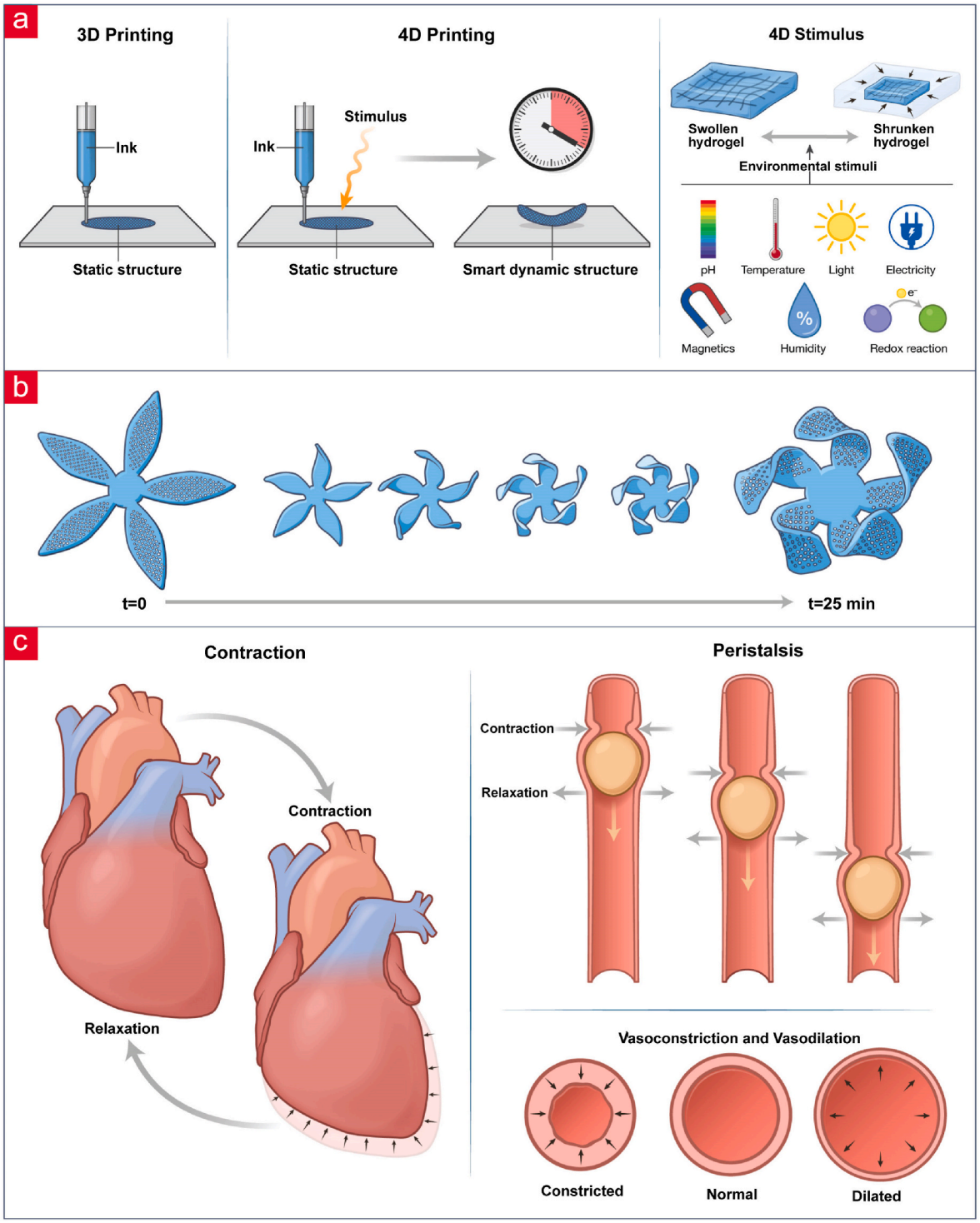

Fig. 1. The concept of 4D printing and it's potential applications in the field. (a) The difference between 4D and 3D printing is depicted her. In simple terms, 4D printed structures can change their 3D configuration over time in response to various stimuli. (b) For instance, 2D flower petals can over time transform into complex flower-like structures. (c) In the body several important tissues are dynamic. Heart contracts and relaxes many times per minute, the process of peristalis pushes food through the gastrointestinal tract, and blood flow inside the body can be controlled via vasoconstriction/vasodilation.

Multi-extruders also sometimes suffer from limitations, such as spontaneous extrusion of materials while the print heads move to a new site, and layer-shifting imperfections caused by the extrusion of different material types on top of one another [9]. Importantly, in 3D bioprinting, the input is a static "material", and the 3D printed tissues are thus not as dynamic as native tissues, including blood vessels, heart, and muscle tissues that change shape over time [12,13].

4D printing has emerged as a possible solution to the above-mentioned challenges. It's based on the beautiful marriage between origami-folding and micropatterned sheets generated via 3D printing (Fig. 1a-b). Specifically, the printed sheets can convolute into highly complex 3D dimensional architectures in response to external or internal stimulus – this is where the fourth dimension, namely time, comes into play [12]. Therefore, 4D bioprinting can create complex shapes with much better resolution without material and cell cross-contamination across different layers and regions [7,9,14]. Besides being able to generate 3D complex shapes with high fidelity, 4D printed structures can also be programmed to respond to stimuli to change their shape and perform pre-determined tasks, exactly like native tissues (Fig. 1c).

Among the hydrogels used for bioprinting, Algs are one of the most investigated due to their high biocompatibility, low cost, and mild gelation process in the presence of divalent cations such as Ca^{2+} and Mg^{2+}. This simple process of gelation turns them into attractive materials for cell encapsulation. Most importantly, the special advantage of Alg is its scalability as it is readily available from various types of brown seaweeds including *Laminaria*, *Ascophyllum*, *Sargassum*, *Alaria*, and *Macrocystis* (Fig. 2). The Alg backbone is also easy to modify chemically and biologically, displays low toxicity towards human cells, and is already frequently used in the clinic with promising outcomes [15–18]. Importantly, for printing applications, Alg pre-polymer solutions display shear-thinning properties (less viscous and flows more easily when subjected to an applied shear force or stress) and are thus desirable precursor materials for the fabrication of 3D printed scaffolds. For these reasons, Algs are the most common building blocks employed in preparing bioinks for bioprinting [7,19]. Unfortunately, unmodified Alg-based scaffolds do not meet some essential needs required by tissue engineering scaffolds because of their mechanical brittleness and low bioactivity (e.g., cell-adhesive moieties) [20]. Neither are they adaptable and dynamic. To overcome these limitations, adaptable Alg bioinks have been constructed via smart chemistry and nanomaterial reinforcement (Fig. 3) [21,22].

This report will specifically review the printing and bioprinting of chemically modified and nanomaterial-reinforced Alg biomaterial-inks and bioinks as well as their applications in both 3D and 4D bioprinting. We will specifically focus on smart Alg bioink based on nanomaterials (e.g., graphene oxide (GO), carbon nanotubes (CNTs), nano clays) [22–24], various chemical groups (oxidized, amines, and methacrylate) [25,26], stimuli-responsive polymers (Poly(N-isopropylacrylamide) (PNIPAAm)), cell adhesive peptide motifs (e.g., Arginine-Glycine-Aspartic acid (RGD), ε-PL, arginine-glutamic acid--aspartic acid-valine (REDV) [27–29], or gelatin (GEL) [30,31] for improving printability and bioactivity. Rheological and mechanical properties will also be discussed. Moreover, we will discuss the development of stimulus-responsive Alg bioinks for 4D printing of living tissue structures, especially through the functionalization of Alg with methacrylate groups. Finally, the recent progress on various applications of such 4D printed Alg-based constructs towards vascularized tissue engineering and cardiac and skin tissue engineering will be described.

2. Development of native-like tissues

2.1. In a nutshell

The demand for tissue or organ transplantation due to donor deficiency and possible rejection of the transplants by the human immune system has prompted the emergence of tissue engineering. Tissue engineering has gained enormous attention due to its potential to restore and repair damaged tissues and organs [32–35]. Cells, scaffolding biomaterials, and growth factors are the main ingredients needed to generate the optimal milieu for tissue regeneration *in vitro* [34,36]. The scaffolding constructs are considered a key factor in the success of tissue engineering [37] since they provide a native-like 3D environment capable of guiding new tissue formation from stem/progenitor cells [5,38]. The most important limitations lie in the fact that most of the scaffolds cannot mimic the complicated architecture and vascular network structure of native tissues [39]. Moreover, only the initial state of the tissue is considered, which is static. These limitations highlight the need for the development of native-like tissues that can mimic both the complex physicochemical properties of native tissues in combination

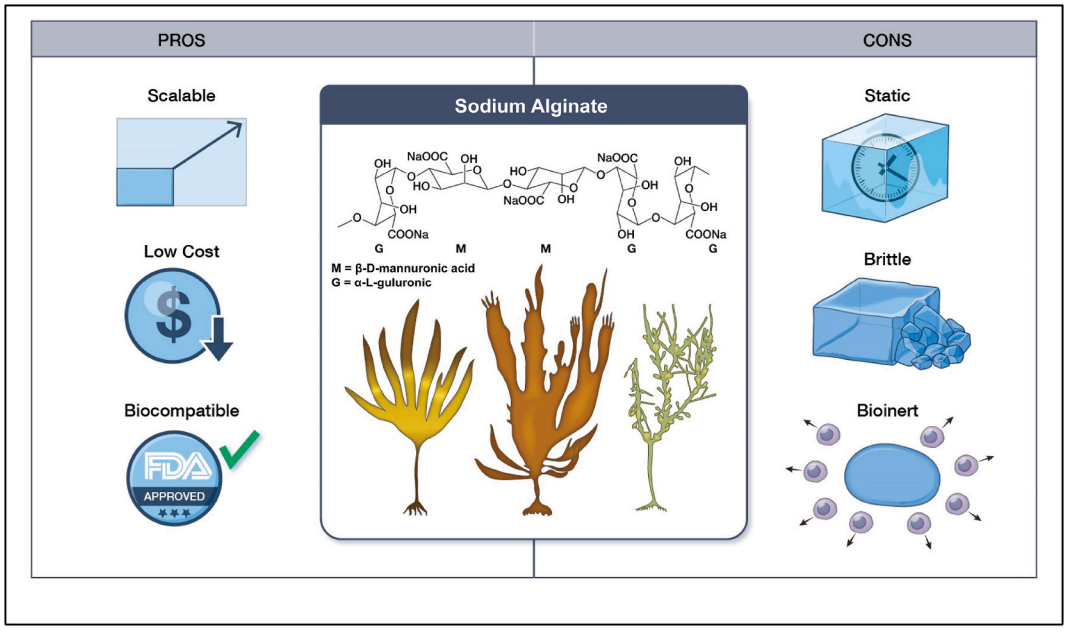

Fig. 2. The various pros and cons of sodium alginate-based inks are highlighted here.

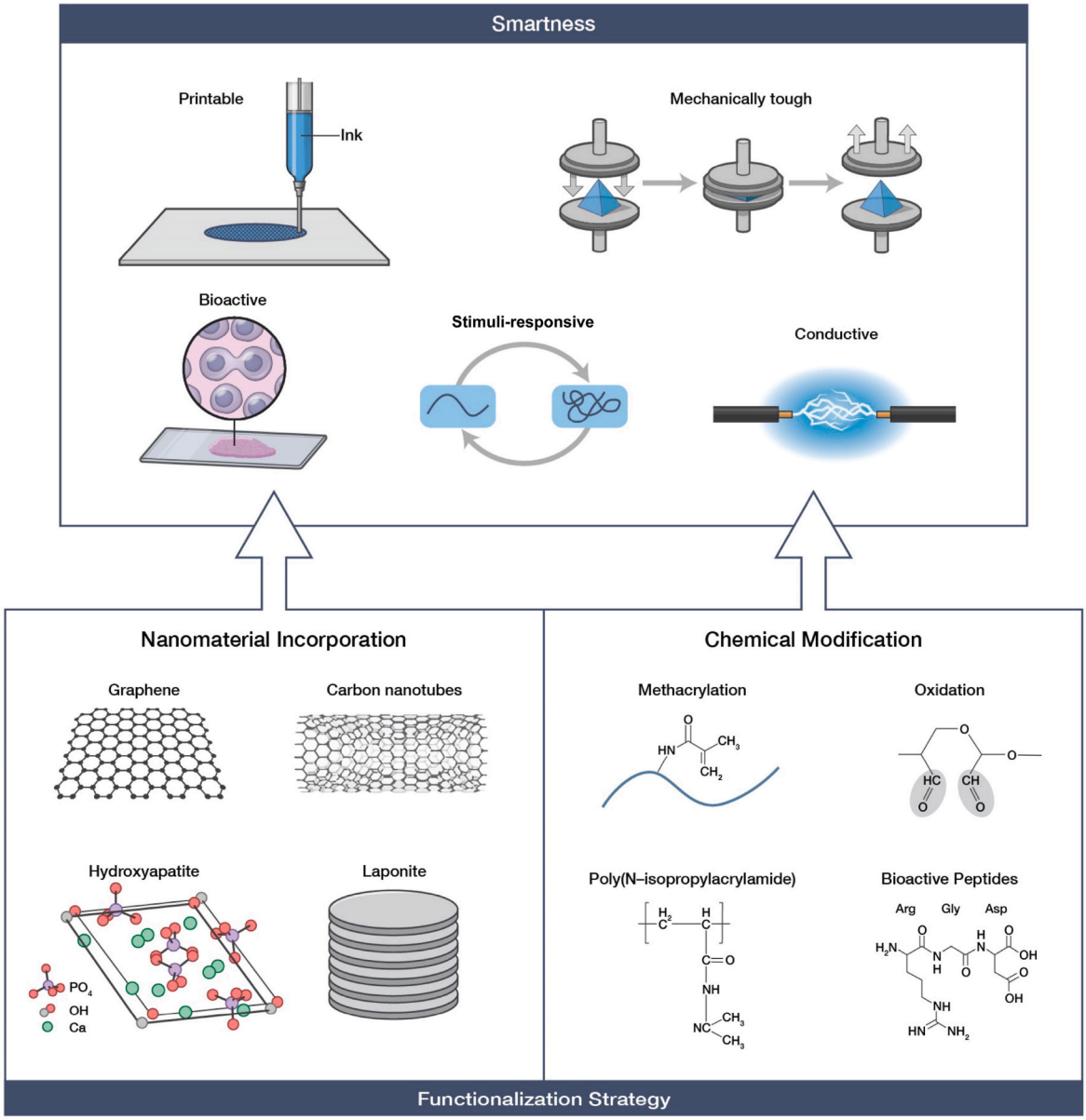

Fig. 3. This figure depicts various strategies for turning conventional alginate inks into smart and dynamic ones applicable for 4D printing. They mostly rely on either nanomaterial incorporation or sophisticated chemical modifications.

with their highly dynamic structure [40–42].

2.2. What's next?

Despite the great promise that tissue engineering holds, certain challenges are associated with this technology, preventing it from spearheading into the clinic. The drawbacks include a lack of renewable and immune-compatible cell sources [43], and biomaterials with desirable mechanical properties and biological activities as well as the inability to generate tailor-made tissue constructs with precisely defined geometries to mimic the complexities of native tissues [5,43]. Biomaterial science has received much attention in the past decade to address these challenges by giving rise multifunctional systems mimicking the chemical, biological, and mechanical properties of native tissues. Recent focus has also been directed toward the research and development of printable biomaterials embedded with cells (BioInks) for 3D printing of tissue engineering constructs that fully embrace the complexity of our tissues and organs [43]. However, most bioinks used for 3D printing are static and therefore not suited for generating dynamic and native-like tissues. With adaptable bioinks, it is now possible to finally deliver off-the-shelf engineered tissues that reproduce the structural and dynamical complexity of native organs. This is possible through 4D bioprinting – an emerging field that details the printing of stimuli-responsive sheets capable of folding into complex architectures over time [36,43].

2.3. Polymeric biomaterials

As mentioned previously, recent developments in tissue engineering have led to a renewed interest in biopolymers [44], as they can serve as tissue engineering hydrogels by providing a 3D porous and wet environment for native-like cell culturing, growth, proliferation, and differentiation [45]. To this end, the tissue engineer must choose the right polymer to match the targeted tissues. The key material properties to consider here are structural, mechanical, and biological. They should also meet several requirements, such as shear-thinning property and

controllable crosslinking ability before they are amenable as bioinks for bioprinting. Indeed, 3D printable polymers for tissue engineering constructs should ideally balance viscosity, stiffness, and gelation time to yield high-fidelity prints [46]. Last but not least, when distinguishing the suitability of polymers for hydrogels, it is important to assess whether they meet key requirements including biodegradability, biocompatibility, and bioactivity [47]. To this end, biocompatibility is one of the most important requirements and refers to the ability of a material to be compatible with the host immune system, while displaying good blood compatibility and sustainable biointegration with the surrounding tissues [48–50].

2.4. 3D bioprinting

The most important limitations of conventional scaffold manufacturing are their inability to construct environments with intricate native-like geometries displaying a localized and well-defined cell distribution. Therefore, there is still room for significant advances that can unleash the entire spectrum of deliverables that might be achieved through tissue engineering [36,51]. To address this grand need in the field, an increasing interest has been dedicated to 3D bioprinting. In simple terms, 3D bioprinting is about accurately placing cell-laden biomaterials in pre-determined 3D hierarchical configurations to develop sophisticated cellular tissue alternatives [36,51]. For this reason, 3D bioprinting has the potential to bridge the current conflict between native tissues and tissue-engineered alternatives [52]. Various bioprinting techniques have been presented based on extrusion, injection droplets, and stereolithography [51]. We will not go into these topics in-depth but will instead refer the interested reader to several excellent reviews [36,51,53–55].

2.5. 4D bioprinting the next big thing?

Despite the success and effectiveness of 3D bioprinting, it has not yet delivered complex structures encompassing multiple cells in combination with different material properties in a convincing manner, exactly like the tissues in the human body [56]. To meet these challenges, 4D bioprinting has emerged as a powerful alternative to the current state-of-the-art [40]. In simple terms, 4D bioprinting is an advanced printing strategy based on 3D bioprinting completed with a fourth dimension (time) that allows the printed constructs to evolve into complicated 3D constructs as a function of time-dependent stimuli [57]. In greater detail, 4D printing is based on printed structures that can change their functionality or/and shape and size with time in response to various external or internal stimuli in a pre-determined way [51,53]. Various physical (e.g., temperature, magnetic and electric field, water), chemical (e.g., pH), and biological (e.g., enzymes) stimuli can be used [57]in this regard.

Moreover, conventional 3D-bioprinted structures follow static patterns and models, where only the initial state of the printed structures is considered. This is contrary to native tissues, which are often based on dynamic alterations caused by external stimuli [51]. For instance, blood circulation throughout the body is regulated by the rhythmic pumping of the heart that is actuated by electric stimuli causing cardiac muscles to contract (Fig. 1c). The same function holds for the musculoskeletal system; however, in this case, the electric stimuli from the nervous system contract the musculoskeletal system, facilitating movements such as walking and running [51]. Another example is the peristaltic movements of the intestine, which consists of successive waves of contraction and relaxation of the smooth muscles of the nutritive wall responsible for directing food along the gastrointestinal tract [56]. Chemical cues or hormones also contribute to how tissues work. For instance, epinephrine or nitric oxide causes vasodilation causing increased blood flow (Fig. 1c) [51]. Therefore, to precisely mimic the function and dynamics of native tissues, it is required to create tissues that can respond to various stimuli by incorporating a time dimension into the 3D printed tissue constructs [51,58]. This can be achieved by incorporating adaptable and stimuli-responsive ingredients.

2.6. Stimulus-responsive polymers

Most stimuli-responsive polymers are either activated by pH or temperature stimuli. We will begin this section by discussing the latter, namely pH-responsive polymers. Amines are the primary groups responsible for making a solution basic (pH $>$ 7.5) and hydroxyls for making them acidic (pH value $<$ 7.5). pH-sensitive polymers are categorized into two groups, polyacids (PAs) or polybases (PBs), with PAs being negative due to carboxylic, sulfonic, phosphoric, and boronic moieties, whereas PBs are positive due to basic moieties, such as various amino-based functional groups. The basic mechanism underlying pH-sensitive polymers is charge-change induced by either proton release or acceptance. This, in turn, facilitates repulsion between like charges and attraction between opposites charges and, ultimately, enables polymers to change their shape.

A hydrated network like those present within hydrogels can also induce hydration or dehydration and thus a shape-change into an expanded or collapsed state, respectively. Several naturally occurring pH-sensitive polymers based on carboxylic (COOH) and amino (NH_2) groups, including chitosan, hyaluronic acid, and carboxyl dextrans or dextran-Amine derivatives, already exist. One might thus rightfully assume that a carboxylic-rich polysaccharide such as sodium Alg is a strong pH-sensitive polymer as well; however, this is not the case, mainly because the zeta-potential of Alg is fairly stable until the pH value reaches around 4, after which it drops slightly and stabilizes again [59,60].

On the other hand, temperature-responsive systems are mostly based on polymers that can change their miscibility as a function of temperature. The lower and upper critical solution temperatures (LCST and UCTS) of the polymer in question are important in this regard, as these boundaries define whether it is miscible or not. At temperatures below the LCST, miscibility occurs, and the contrary is the case at temperatures higher than the UCTS. Importantly, the polymer is expanded and highly hydrated in the high miscibility range, whereas it enters a collapsed and highly hydrophobic state in the low miscibility regions. The concept here is thus pretty similar to the one based on pH-value changes as they are intimately linked with changes in system hydration. One of the most widely used polymers in this direction is Poly(N-isopropylacrylamide), or in the abbreviated form PNIPAAm. PNIPAAm exhibits an LCST value at 32 °C and, therefore, becomes extremely dense at body temperature. Since it also contains amine groups, it simultaneously gives rise to pH responsiveness and is, therefore, one of the most preferred stimuli-responsive polymers.

It is also worth noting that some stimuli-responsive hydrogels are possible as well through dynamic bonds. These hydrogels are highly dynamic since they can change their structure under various stimuli [61]. Some of the dynamic covalent bonds that have gained attention in this regard are acylhydrazone, imine, and disulfide bonds because they are highly pH-sensitive and can exhibit sensitivity toward various biological and chemical stimuli [61]. For instance, acylhydrazone bonds can easily hydrolyze in the presence of acidic media; however, they are stable in basic and neutral conditions. Imine bonds, which typically are based on dynamic covalent bonds between aldehydes and amines display similar pH-sensitive as hydrazone bonds.

Biomedical engineers have, over the years, used the abovementioned dynamic crosslinks and chemical groups to control the hydration degree of hydrogel-like materials, and thereby the shape of the system in question since this property is intimately linked with the matrix crosslinking density. Indeed, as the crosslinking density decreases due to, for instance, pH-mediated bond rupturing or repulsion, the swelling degree will, in most cases, increase concomitantly. For this reason, systems based on the above chemistries can endow shape-changing properties to 3D printed systems. Imagine a 3D printed structure in which different

regions in the prints give rise to different swelling ratio changes in response to pH value. What would happen if this value was gradually changed over time? What would happen if some regions would increase their swelling while others experienced decreased hydration in response to this kind of stimuli? In such a scenario, conflicting forces across the 3D printed construct will facilitate some sort of heterogeneous shape changes. As recent studies have shown, one can easily, by using modeling tools, predict how to 3D print multiple stimuli-responsive materials in beforehand-predicted patterns that, in response to proper pH-stimuli, can yield pre-determined 3D architectures over time [62,63]. This review paper will center its attention on Alg, which stands out as a highly promising type of natural polymer for creating stimulus-responsive hydrogels.

3. Alginate's properties

Alg is an anionic polysaccharide extracted from brown seaweed [18,64,65] containing blocks of (1,4)-linked β-D-mannuronate (M) and α-L-guluronate (G) residues (Fig. 2) [18,46,66]. The negative charge on Alg has been attributed to carboxyl groups within its backbone [67]. The physical properties of Alg hydrogels are mostly affected by molecular weight and negative charge. Indeed, it is the negative charge of Alg that facilitates ionic crosslinked hydrogels via divalent cations such as calcium-mediated physical bonds between adjacent Algs [68], whereas Alg's with higher molecular weight typically give rise to hydrogels with higher mechanical stiffness.

Another important factor besides charge and molecular weight is the ratio between G and M blocks. Depending on the origin, the G content of Alg can vary between 10% and 70%, something detrimental in defining the quality of the Alg in question [69]. Briefly speaking, G blocks are involved in intermolecular crosslinking facilitated by divalent cations, and therefore its presence in the Alg backbone plays a key role in hydrogel formation and its stiffness – as more crosslinking results in stiffer hydrogels. In contrast, high M content gives rise to more flexible Alg hydrogels due to less rigidity than G blocks [18] For this reason, the mechanical properties of Alg hydrogels can be fine-tuned by modulating the G:M ratio and molecular weight – with higher molecular weight and G:M ratio typically resulting in mechanically stiffer hydrogels [70].

3.1. Pros and cons

Alg is a natural polymer that displays several exciting properties, including biocompatibility, scalability, high availability, solubility, low cost, feasible gelling time, shear-thinning capability, low toxicity, and tunable pre-hydrogel viscosity (Fig. 2) [18,71,72]. Most importantly, it can provide a proper niche for cells as it resembles another polysaccharide in the native ECM – hyaluronic acid – moreover it can simultaneously act as a suitable immuno-protective barrier for their delivery into the body [73–75]. It can simulate a niche that offers specific external conditions for cell attachment, proliferation, differentiation, as well as migration, thereby promoting tissue regeneration. The benefit of using these materials lies in their resemblance to the ECM found in natural tissues, often eliciting responses resembling those in the body under normal conditions such as biodegradation [73].

As mentioned above, the main limitations associated with today's biomaterials are lack of scalability, biocompatibility, and FDA approval. To this end, Alg is a promising candidate since it has several attractive features, especially excellent biocompatibility, scalability, and structural resemblance to natural ECM [46]. Notably, it has been used for decades in clinical applications, such as cell encapsulation to treat heart disease, diabetes, neurodegenerative disorders, myocardial repair, and more [76]. For these reasons, Alg is one of the most promising hydrogel biomaterials in the field of tissue engineering and will thus be the main focus of this review paper.

However, there is growing concern about using Alg in tissue engineering due to its brittleness and the lack of cell-adhesive motifs within its backbone – factors that are essential for cell proliferation and adhesion [40,46,77,78]. These limitations can be overcome through the functionalization of Alg with bioactive materials, such as cell adhesive motifs (e.g., RGD and IKAV) or with another natural biopolymer, such as gelatin (GEL) [79,80]. Moreover, by modifying Algs with oxidized and methacrylate groups, their biodegradability and printability can also be improved [37,79]. Furthermore, mechanical, rheological, electrical, and biological properties, as well as printability, can be improved by incorporating conductive or mineral-based nanomaterials, such as graphene oxide, CNTs, nano clays (Laponite®) into the Alg matrix [5,6,78]. This will be further addressed in Section 4.

3.2. Printability of alginate

The building blocks of 3D-bioprinted constructs are called "bioinks". They, in brief, consist of a wet encapsulating material – typically a hydrogel – and cells, sometimes together with growth factors and drugs. Importantly, they need to be printable and thus have to exhibit sufficient liquidity to flow through the printer head. They must also solidify within seconds to maintain a predefined shape in a post-print scenario [81]. This is sometimes difficult to fine-tune, and for this reason, shear-thinning bioinks are receiving increasing attention.

Shear-thinning implies that a viscous and solid-like bioink can become liquid-like in the presence of extrusion shear and quickly return to its original state after printing. The shear-thinning property is mainly based on reversible polymer-polymer interactions, such as hydrophobic, hydrogen, and electrostatic bonds [82]. Since Alg bioinks are based on reversible electrostatic interactions mediated by calcium ions, they display good shear-thinning properties. Indeed, by blending Alg solutions with multivalent cations, hydrogels are formed rapidly due to ionic intermolecular bonds. This also allows cells to rapidly become encapsulated without unwanted sedimentation and subsequent heterogeneous cell distribution.

Other significant advantages make Alg an appealing bioink material, such as easy tunability of hydrogel pore size, mechanical stiffness, viscosity, and shear-thinning properties. The fine-tuning can be accomplished by simply adjusting the G:M ratio, concentration, and molecular weight [7]. Overall, due to the extra versatility, scalability, gelling capacity, and printability of Alg materials, they are currently considered among some of the most promising hydrogel systems for 3D and 4D printing. However, one of the hurdles that must be overcome before 4D printable Alg hydrogels can become a reality is finding scalable and feasible methodologies to turn an otherwise not stimuli-responsive polymer into something that is sufficiently responsive for enabling 4D printed constructs. We will discuss this challenge in greater depth in the following section.

4. Smart alginate BioInks

Preparing smart Alg inks involves the modification and combination of Alg with multiple materials using smart chemistry and nanomaterial reinforcement. This process results in the creation of Alg bioinks with unique properties such as enhanced bioactivity, printability, and mechanical strength. In this section, we will discuss various strategies for modifying Alg bioinks. These strategies include incorporating conductive or mineral-based nanomaterials, as well as chemical modifications such as metacrylation and oxidation. Additionally, we will explore the functionalization of Alg bioinks with cell adhesive motifs and biopolymers like GEL. Furthermore, we will examine the impact of these approaches on the properties and bioactivity of Alg hydrogels.

4.1. Nanomaterial reinforcement

Carbon-based nanomaterials, including GO, reduced graphene oxide (RGO), single-walled carbon nanotubes (SWCNTs), and multi-walled carbon nanotubes (MWCNTs), are frequently used as nanoreinforcers

in Alg hydrogel bioinks as they can give rise to improved mechanical strength, electrical properties, thermal conductivity, and biological properties [24,78,83,84]. Moreover, recent studies have reported that they are biocompatible while simultaneously being able to enhance the printability of a wide range of hydrogels, including Alg-based hydrogels [22,23,85].

Due to the many promising properties of carbon-based nanomaterials, they are currently widely used for biomedical applications, including drug delivery, tissue engineering, and biosensing [83]. As an example of the beneficial properties of GO inclusion into Alg, we have highlighted a recent study by Li et al. [86] Here, the authors incorporated GO into the Alg matrix through a simple design and mixing procedure in the presence of calcium chloride. In brief, by adding GO into the Alg solution, GO functional groups such as (-OH, and –COOH) interacted with Alg (-OH) groups leading to the formation of hydrogen bonds between Alg and GO, while the calcium ions facilitated electrostatic bonds between adjacent Algs. A series of rheological experiments confirmed that GO inclusion improved the shear-thinning properties of the composite system [86]. The authors speculated that the observed improved shear-thinning property was linked to reversible hydrogen bonds between the hydroxyl groups within the Alg backbone and on the GO surface. Due to the enhanced shear-thinning properties, GO-reinforced Alg biomaterial inks gave rise to better prints, as evident from the resolution of the prints, which decreased from about 0.43 to 0.25 cm as the GO concentration increased from 0 to 0.25 wt%.

In a similar study, Choe et al. [78] developed Alg-GO composite bioinks by mixing Alg to obtain 3 w/v% Alg and different GO concentrations (0, 0.05, 0.25, 0.5, and 1.0 mg mL^{-1}). Mesenchymal stem cells (MSCs) were encapsulated in the ink, and then, the composite scaffolds were bioprinted and crosslinked by immersion in a 90 mM calcium chloride solution for 5 min, followed by washing with sodium chloride solution. It was observed that by increasing the concentration of GO from 0 to 1 mg ml^{-1}, the viscosity increased from 146.9 ± 4.8 Pa S to 189.2 ± 0.1 Pa S (Fig. 4a). Notably, all the tested Alg-GO bioinks exhibited improved shear-thinning properties compared to pristine ones. Moreover, the mechanical properties (shear moduli) of Alg ink reinforced with 1 mg ml^{-1} GO (Alg-GO-1) were reported to be 1.23-times higher than those of pristine inks, as observed in Fig. 4 b [78]. The improved mechanical properties were attributed to intensified hydrogen bonds due to strong interactions between Alg and GO. Especially, it was found that composites with higher GO concentration resulted in better printability due to observed thinner strands in 3D printed scaffolds (Fig. 4c). The cell's viability was examined, and the majority of cells within the scaffolds were deemed viable post-printing. The results of the viability assessment demonstrated that all Alg-GO bioinks and printing methods were appropriate for 3D bioprinting. Furthermore, extended cultivation of these cell-laden scaffolds in a growth medium maintained their viability for a duration of 7 days. Regarding bioactivity, the Alg-GO-0.5 bioinks composed of 0.5 mg mL^{-1} GO and 3 w/v% Alg gave rise to the most optimal expression of

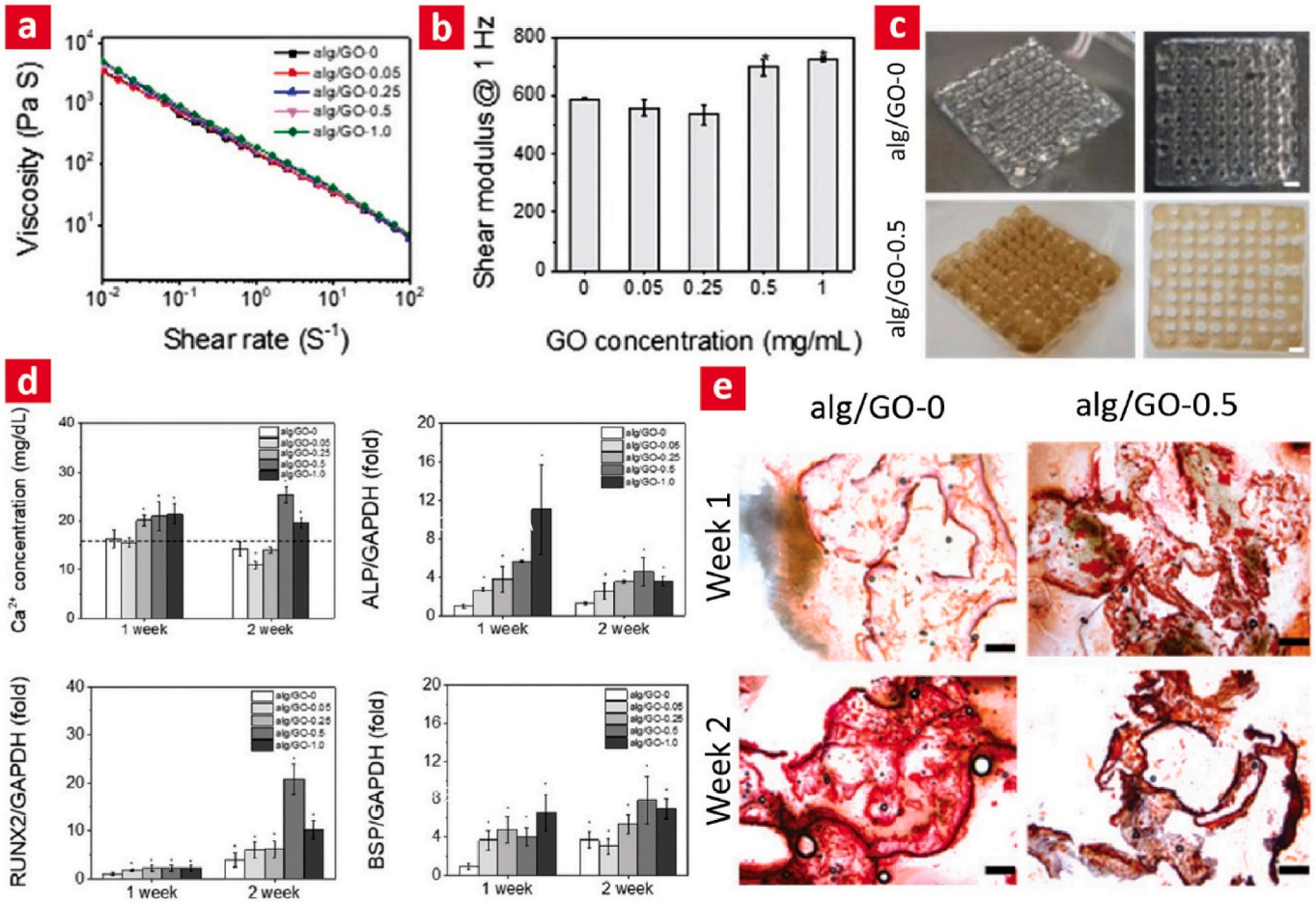

Fig. 4. Osteogenic and mechanically tough Alg prints based on GO-incorporation. (A) The shear-thinning properties as function of GO-incorporation is shown here. (B) The shear modulus increased concomitantly with GO content. (C) Strands were thinner and print fidelity much better after 0.5 mg/ml GO incorporation. (D) Bone mineralization and the expression of osteogenic related markers was in general highest after either 0.5 or 1.0 mg/ml incorporation. (E) After two weeks Alizarin Red S staining against calcium showed no differences between pristine and GO-incorporated gels. However, after 1 week the presence of calcium increased as function of GO content. Adapted with permission [78]. Copyright Royal Society of Chemistry, 2019.

osteogenic markers from encapsulated mesenchymal stem cells (Fig. 4d-e). The authors speculated that this was most likely linked to the osteogenic capacity of GO, as reported in previous studies [78,79,87].

Another carbon-based nanomaterial, CNT, has also greatly benefited Alg in 3D printing. For instance, in a recent study by Li et al. [85] the authors prepared a hybrid Alg and GEL biomaterial ink doped with CNT through a simple design, mixing, and dispersing procedure. Specifically, the Alg-GEL-CNT biomaterial inks were extruded from the nozzle into a rotating cylinder to print vascular scaffolds. A syringe sprayed the calcium chloride on the printed tubular scaffolds to pre-crosslink them during the printing. Afterwards, the scaffolds were completely crosslinked by immersion in calcium chloride solution for 30 min. It was observed that the viscosity of the Alg-GEL scaffolds increased after crosslinking; as expected, the Alg-GEL-CNT scaffolds exhibited improved shear-thinning properties, making them easier to print. Additionally, the mechanical properties of the printed scaffolds doped with 0.5% CNT were reported to be the highest. For instance, Young's modulus increased from 0.156 MPa to 0.898 MPa as the CNT concentration increased from 0 to 0.5% (w/v). However, Young's modulus of the scaffolds doped with 1% CNT was lower than that of the 0.5% CNT scaffolds. The cell adhesion coverage on the other hand decreased from 90.12 + 5.90% (0% CNT) to 77.55 + 4.00% (0.5% CNT) and finally 24.28 + 6.00% (1.0 CNT %). The reason was that the existence of CNT strengthened the rigidity of the scaffold and reduced the roughness of the inner and outer walls, which made it tough for cells to adhere to the surface and inside of the scaffolds in a short time. We speculate that this could be correlated with CNTs being non-toxic for mammalian cells at really low concentrations, and 0.5% might be the critical safe limit in the current study [5]. Also, in another study, Suo et al., printed porous scaffolds using a combination of CNT, chitosan, and Alg materials. The viability of human periodontal ligament cells (hPDLCs) on these scaffolds was assessed. Their results revealed that the scaffold containing 0.5% CNT exhibited the highest level of biocompatibility. This suggests that a CNT concentration below 1% can enhance hPDLC proliferation [88]. Overall, the results demonstrated that Alg-GELs doped with 0.5% CNT were the most optimal in terms of mechanical and biological properties, while higher concentrations elicited non-ideal biological properties. For these reasons, proper content control of CNT doping is essential to improving the mechanical and rheological properties of 3D printed scaffolds to assure minimal impact on cell cytotoxicity [85].

In conclusion, carbon-based nano-reinforced bioinks have added exciting attributes to pristine Alg bioinks, such as improved printability and print fidelity, increased mechanical strength, improved osteogenic differentiation, and cell attachment. For these reasons, the inclusion of carbon-based nanomaterials in the field has paved the way for some exciting scientific possibilities. However, sometimes these fail when the nanomaterial concentration reaches a critical limit. Accordingly, a proper dose-response test is necessary for such studies to secure the most optimal formulation for further downstream studies.

4.1.1. Mineral-based

Mineral-based nanomaterials, such as hydroxyapatite (HAP), and nanoclays such as Laponite®; synthetic clay made of lithium sodium magnesium silicate, are attractive Alg bioink reinforcing candidates not only because of their inherent osteogenic potential but also due to their ability to enhance mechanical properties and printability [20,24,89,90]. For this reason, nanoclays are among the most extensively used nano-reinforcements that have been incorporated into Alg to prepare bioinks [83]. This is intimately linked to their high biocompatibility, good solubility in water, potent effects on mechanical and shear-thinning properties, as well as a beneficial impact on musculoskeletal cell behavior due to their mineral dissolution products, including Li, Mg, Si, Al, and Na [83].

Dávila et al. [91] explored these desirable material properties by manufacturing a Laponite®-Alg ink through a simple design, mixing, and dispersing procedure. They later used them for extrusion-based 3D printing. Initially, the laponite® was dispersed in deionized water by a vortex stirrer. Afterwards, they mixed laponite® with an Alg solution and stirred it to ensure uniformity. Subsequently, the extruded inks were ionically crosslinked by immersion in a 0.1 M calcium chloride solution for 24 h to make them fully crosslinked. It was shown that in the laponite®-Alg system crosslinking was facilitated through reversible electrostatic interactions between the anionic Alg and the positive rim charge of laponite® platelets. Accordingly, laponite® reinforcement gave rise to better shear-thinning behavior because of these physical bonds and thereby a better printability than pristine Alg. To this end, Alg alone behaved liquid-like, unlike those containing 2 wt% laponite®, which exhibited a more solid and viscoelastic behavior, while laponite® with a concentration of at least 5 wt% exhibited the best printability as assessed through shear viscosity measurements. For these reasons, the laponite®-Alg showed a high ability to maintain its shape after printing due to its solid-like behavior and subsequent rapid viscosity recovery after the extrusion printing phase [91].

In a similar study by Jin et al. [92] the authors pushed this concept further by printing more complex Alg-laponite® hydrogels. Like in the previous study, the authors mixed laponite® with Alg and demonstrated that the biomaterial inks could be printed into 3D scaffolds directly, while maintaining their shape even before crosslinking. For instance, laponite-Alg composite hydrogel precursors were extruded into highly complex, multilayered cups and tubular structures. Indeed, during the printing phase, the laponite®-Alg printed structures retained their as-deposited shape without additional support. After the deposition of an entire cup structure, the printed hydrogels were physically crosslinked by calcium chloride. In addition to enhanced printability, laponite® improved the printed Alg's mechanical and biological properties. Notably, Young's modulus of these hydrogels increased 7.4-fold as the laponite® concentration increased to 6% (w/v) compared to the unmodified hydrogels, while their resistance to degradation in cell culture medium, and cytocompatibility made them suitable hydrogels for widespread use *in vivo* and *in vitro* studies [92]. For these reasons, it was concluded that adding laponite® could promote the printing of Alg hydrogels and improve their mechanical properties.

Some studies have also taken advantage of HAP nanomaterials to facilitate 3D-printed constructs with good mechanical and biological properties [20,93–95]. For example, Liu et al. [20] fabricated microporous scaffolds based on 3D printing of Alg-HAP biomaterial inks. Initially, they added HAP nanoparticles to deionized water and stirred it for 2 h to obtain a uniform slurry. Subsequently, they added Alg to the previous slurry and stirred that one for 3 h to obtain an Alg-HAP suspension. Next, D-Gluconic acid δ-lactone (GDL) was added to the above suspension to form pre-crosslinked Alg-HAP hydrogel. The pre-crosslinked hydrogel ink was extruded via 3D printing into porous scaffolds and then immersed in 10 wt% calcium chloride solution to facilitate additional crosslinking. After this crosslinking step, the scaffold was removed and freeze-dried for further downstream studies. Notably, the mechanical properties of the finalized porous scaffolds were improved by increasing the HAP content to 7 wt%. To this end, the compressive strength of Alg-HAP scaffolds was reported to increase about 8.5 times as the HAP concentration increased from 1 to 7 wt%. Finally, the authors demonstrated that the HAP nanoparticles could improve the mechanical strength of the 3D-printed scaffolds. The main reason was attributed to the greater stress transferred from the Alg matrix to the rigid HAP nanoparticles, thereby enabling an additional energy dissipation pathway in the system. Additionally, *in vitro* results demonstrated that increasing HAP concentration to 7 wt% HAP resulted in improved cell adhesion and proliferation. It was thus concluded that neither low nor high HAP concentration favored cell adhesion and proliferation, but a medium HAP concentration did.

Despite laponite®'s great promise in improving the printability of Alg bioinks, there are still few papers on the impact of other mineral-based nanomaterials on improving the Alg bioinks. Therefore, further research is needed to evaluate the capability of other mineral

nanoreinforcements to improve the various properties of Alg bioinks. The above systems were also static and thus not suitable for 4D printing. Indeed, in our opinion, these systems need more attention to fully open up this field in the coming years, and we look forward to further developments dealing with dynamic Alg hydrogels achieved via nanoreinforcement.

4.2. Functionalized alginate

Functionalized Alg can provide exciting properties to Alg bioinks such as improved printability, mechanical properties, stimuli-responsiveness, bioactivity, and controlled degradation. For instance, the functionality of Alg can be improved through the incorporation of aldehyde and methacrylate groups, PNIPAAm, cell adhesive peptides, and GEL. In the following sections, we have reviewed these functionalization strategies and the properties they can bestow upon pristine Alg [83,96,97].

4.2.1. Alginates functionalized with cell adhesive peptides

Unfortunately, Alg has no adhesive ligands for anchoring cells. Something which, in turn, results in poor cell adhesion, proliferation, and differentiation. Even though nanomaterial reinforcement and backbone modifications with methacrylate and oxidize groups are beneficial, they cannot induce cell spreading and proliferation as they lack receptors that can bind to the cell membrane integrins. Cell adhesive peptides can be considered a potential route to improve tissue regeneration [83,97]. To stimulate cell interaction, bioactive cell adhesive peptides such as RGD, YIGSR, and IKVAV peptides have been covalently linked to the Alg backbone to improve cell adhesion, proliferation, and viability [97,98]. Indeed, these peptides have, over the years, been used to induce cell attachment in artificial systems and mimic native-like cellular. A minimum concentration of cell adhesives peptides in alginate gels is needed for the adhesion and growth of cells, and this minimum is probably cell-type specific. The typical approach for alginate modification using bioactive peptides involves incorporating peptides at a concentration of 0.1–1.0% per mole of uronate monomer. Indeed, peptide densities within this range do facilitate the adherence of myoblasts, olfactory ensheathing cells, mesenchymal stem cells, and endothelial cells [77].

RGD has been widely studied in this direction due to its availability and ability to attach to a wide range of integrins [29,77]. For instance, Genes et al. [99] developed RGD-functionalized Alg hydrogels and subsequently examined the attachment of chondrocytes to them. The results demonstrated that chondrocytes attachment to RGD-Alg was 10- to 20-times greater than that of unmodified hydrogels. Importantly, it was found that RGD functionalization allowed the attachment of chondrocytes to Alg through the involvement of integrins, especially β_1 and α_3, as well as the actin cytoskeleton. The authors also found that chondrocytes were rapidly attached to Alg substrates by increasing the RGD density.

Huebsch et al. [100] developed a similar Alg matrix and examined the behavior of mesenchymal stem cells (MSCs) within them. These authors demonstrated that encapsulated MSCs within such 3D matrices used α_5 integrins as RGD receptors. To this end, they discovered a correlation between α_5-RGD binding, elastic modulus, and osteogenic commitment. Notably, the expression of collagen I and osteocalcin secretion became considerable after 1 and 3 weeks, respectively. This suggested that bonds between MSCs integrins and RGD could facilitate an osteogenic commitment.

Solano et al. [101], created and characterized an Alg-based hydrogel functionalized with RGD, aiming to potentially trap cancer cells. Analysis using microcomputed X-ray tomography revealed that the hydrogel structures consist of interconnected pores with an average diameter of 300 μm. The F98 glioblastoma (GBM) cells migrated within these pores, gathering predominantly at the center of the structure. Depending on the initial number of cancer cells, introducing RGD cell-adhesion peptides to the Alg led to a 4 to 10-fold increase in the retention of F98 cells (which excessively express the associated αvβ3 and αvβ5 binding integrins) within the structure.

Tan et al. [102] exhibited that human nucleus pulposus (NP) cells cultivated on or within Alg hydrogels functionalized with cRGD (integrin-binding) and AG73 (syndecan-binding) peptides displayed enhanced cell attachment, viability, biosynthetic activity, and expression of NP-specific characteristics compared to Alg alone. Each adhesive peptide had a distinct impact on cell attachment, appearance, formation of focal adhesions, and subsequent effects on biosynthesis, which were newly unveiled for NP cells. The combined presence of both peptide types induced markers characteristic of the NP-specific cell phenotype, including N-Cadherin, despite differences in cell shape and the tendency to create clusters of multiple cells in both 2D and 3D culture settings. These findings are a promising stride toward comprehending how unique adhesive peptides can be merged to guide the destiny of NP cells within the established 3D Alg culture, potentially aiding the rational design of hydrogels for NP cell-transplantation-oriented therapies targeting degenerated intervertebral discs (IVD).

Despite these promising results, the above functionalizations are mono-functional modifications as they only improve bioink bioactivity. But what about printability, controlled degradation, and mechanical and electrical properties? Unfortunately, this is only possible if the cell adhesive peptides are combined with for instance either OMA or nanomaterials, which almost certainly will give rise to their fair share of drawbacks because of the many consecutive and difficult functionalization strategies needed here.

4.2.2. Alginate functionalized with gelatin

Another alternative approach to improve the bioink bioactivity of Alg is to functionalize it with GEL – a widely recognized bioactive protein derived from hydrolyzed collagen [96]. Due to the similar composition of GEL to collagen (an essential component of the ECM), it displays important cell adhesive sequences and is, therefore, widely used for tissue engineering applications [103]. Importantly, combining GEL with other polymers such as Alg can enhance other important properties besides bioactivity, including improved shear-thinning and mechanical properties. Especially in combination with oxidized alginate (OA), GEL can, through its abundant amino groups, establish dynamic imine bonds with the OA backbone [96]. Since dynamic covalent bonds are reversible, the right mixture of OA and GEL can yield shear-thinning and self-healing systems simultaneously – which is equally important for generating good prints.

The benefits of shear-thinning for 3D printing applications have been touched upon several times throughout this review; however, for some readers, the correlation between printability and self-healing might not be as obvious since this is a relatively new concept in the field. Briefly, a self-healing polymer can be extruded as an intact material even if it has already passed the liquid and viscous phases and entered a more solid-like phase. This can facilitate higher fidelity prints since the printed materials' flowability, and associated dispersion are reversibly correlated with post-print bioink elasticity. Indeed, solid-like hydrogels that exhibit zero post-print material spillover can only be printed via tremendous shear forces leaving ruptured 3D prints. In this regard, the key advantage of self-healing is that it enables the restoration of such crumbled post-print materials to yield homogenous and smooth structures.

Along these lines, Soltan et al. [31] synthesized OA-GEL hydrogels and evaluated their cell viability and printability. In brief, GEL was gently added to the OA solution to facilitate a hydrogel via dynamic and covalent imine bonds. Before bioprinting, the OA-Gel mixtures were allowed to covalently gel for more than two nights in the refrigerator. The authors evaluated the printability of the inks by considering four printing factors, including extrudability, uniformity, and structural integrity. To this end, they found that the OA-GEL hydrogels with final concentrations of OA(2 w/v%)-GEL(2 w/v%), OA(2 w/v%)-GEL(3 w/v

%), and OA(3.75 w/v%)-GEL(3.75 w/v%) gave rise to the best prints due to better shear-thinning compared to the OA(6 w/v%)-GEL(2 w/v %), OA(3 w/v%)-GEL(2 w/v%), and OA(2 w/v%)-GEL(6 w/v%) groups (Fig. 7) [31]. The pore factors of various groups were assessed after printing two layers. Similar to the uniformity factor, the inclusion of a cross-linker enhanced the pore factor measurements. For instance, the pore factor associated with the OA(2 w/v%)-GEL(2 w/v%) (2|2) group significantly improved from initially coalesced and absent pores to a pore factor at 1.04. All groups except for OA(2 w/v%)-GEL(6 w/v%) (2|6), achieved a favorable uniformity and pore factor close to 1 when printed with a cross-linker [31].

In a similar study, Jiang et al. [30] developed Alg-GEL hydrogel inks by mixing GEL with Alg and stirring the solution for 3 h to ensure uniformity. These hydrogel precursors were heated to 37 °C to obtain homogenous solutions. Subsequently, the precursors were mixed with breast cancer cells and subsequently stored at room temperature to allow gelation to be initiated before the printing process. The bioprinted hydrogels were crosslinked by immersion in a 100 mM calcium chloride solution. Besides Alg crosslinking via calcium ions, the authors also speculated that additional interactions between Alg and GEL might be present, such as imine, and electrostatic bonds [104]. Notably, it was observed that Alg-GEL hydrogels with low Alg and high GEL concentrations exhibited a soft mechanical structure with more cell-adhesive moieties, which in turn facilitated higher cell viability and the formation of tumor spheroids. On the other hand, hydrogels with high Alg and low GEL concentrations showed stiffer structures with lesser cell-adhesive moieties and, therefore, lower cell proliferation rates. Additionally, it was found that the viscosity increased by increasing either the GEL or Alg concentration – this, in turn, led to a higher resistance to shear flow, resulting in lower flow rates. Specifically, the authors concluded that A1G7 (here, the Alg and GEL concentrations were 1% and 7%, respectively), and A1G9 (here, the Alg and GEL concentrations were 1% and 9%, respectively) hydrogels were the best samples from a 3D Bioprinting perspective. They exhibited both high biofunctionality and printability and could be bioprinted rather quickly (within 30 min) without any adverse effects on cell viability and proliferation.

Overall, we conclude that despite all the advantages of the discussed Alg-based inks for 3D bioprinting, neither Alg-GEL nor Alg-peptide hydrogels can be used for 4D printing due to their inability to respond to stimuli. Even though some of the OA and OMA hydrogels could, in principle, be made 4D printable, they were not sufficiently stimuli-responsive and gave rise to their fair share of challenges and drawbacks. For this reason, there is a need to identify alternative methods to prepare stimuli-responsive Alg bioinks for 4D printing. Something which we will discuss in more depth in the following section.

4.3. Stimulus-responsive Alg systems with static and dynamic bonds

In this section; we will explore possible methods to make Alg inks more adaptable for down-stream 4D printing applications by either including a stimuli-responsive network alongside its network or modifying its backbone with a stimuli-responsive moiety [105].

4.3.1. Methacrylated and oxidized alginates

Alg has frequently been modified through methacrylation to control hydrogel degradation and mechanical properties. For instance, in a recent study, Mishbak et al. [21] doped the Alg backbone with photoreactive methacrylate moieties and observed that with increasing degrees of photoinitiator, the mechanical stiffness of the hydrogels and their degradation rate increased, while the gelation time and hydrogel pore size decreased. These functionalization strategies can also improve printability either directly or indirectly. For instance, 3D-printed methacrylated Alg can immediately crosslink via UV light to avoid material spillover and layer impurities [83].

By oxidizing Alg several exciting properties have been observed. Indeed, several studies have demonstrated a correlation between the printability, density, and viscosity of OA solutions [106–108]. The same study also established an intimate link between hydrogel degradation, mechanical strength, and oxidation. All the OA samples exhibited better biodegradation properties than non-oxidized Alg samples. These authors also found that the good printability of OA bioinks was intimately linked to their capacity to maintain a homogenous 3D cell distribution after bioprinting. Indeed, they discovered that good homogeneity could be maintained with a biomaterial density equaling or being higher than the density of the investigated cell type – something attributed to the relatively high viscosity from the point-of-view of cells when embedded in such solutions, as this can significantly slow down cell movement and prevent sedimentation. By increasing the oxidation degree, they could also lower the density and viscosity and vice versa. To this end, they observed that bioinks with a density of 1.05 g cm^{-3} (similar to most cell solutions) sustained a homogeneous hADSCs suspension for up to 3 h after bioprinting without notable cell sedimentation. Finally, the authors reported that the viscosity increased with increasing Alg concentration or decreasing degree of oxidation. Importantly, the optimal viscosity range for 3D bioprinting of this system was determined to be about 400 mm^2 s^{-1} to 3000 mm^2 s^{-1} [106].

Some studies have also combined the two functionalization approaches [109–111]. For instance, Jeon et al. [109] synthesized oxidized and methacrylated Alg (OMA) hydrogels (Fig. 5a). The OMA macromer was developed by reacting OA with 2-aminoethyl methacrylate to provide OMA at a 45% methacrylation degree. To prepare photo-crosslinked OMA hydrogels, the OMA solutions (2, 4, and 8 w/v %) were inserted between two glass plates and then photocrosslinked with UV light for 15 min. In this regard, they demonstrated that they could control degradation, swelling, and mechanical properties of the crosslinked hydrogels by simply tuning the OMA oxidation degree [109,111]. Importantly, the storage moduli (elastic part) of OMA hydrogels (4 w/v %) were considerably higher than the loss moduli (viscous part) for all degrees of Alg oxidation. As the oxidation degree of the Alg increased from 9% to 20%, the storage moduli decreased from 4693 ± 691 Pa to 879 ± 112 Pa, as seen in Fig. 5 b [109]. One can thus argue that a higher Alg oxidation degree results in less elastic hydrogels – something plausibly attributed to the inverse correlation between molecular weight and oxidation degree. Additionally, the swelling of OMA hydrogels with an oxidation degree of 9% decreased by increasing the OMA content to 8 w/v% (Fig. 5c-d). Indeed, these hydrogels reached equilibrium swelling within 1 week and then maintained a constant hydration degree for 4 weeks. Increasing the oxidation degree from 9% to 14% allowed faster swelling kinetics. Here, the swelling of OMA hydrogels with an oxidation degree of 14% reached a maximum by day 1 (2 and 4 w/v %) or 1 week (8 w/v %) and then rapidly decreased with degradation [109]. Finally, the authors demonstrated that the functionalized Alg hydrogels improved cell proliferation and adhesion compared to the pristine hydrogels (Fig. 5e). Specifically, hydrogels using lower polymer concentrations (2 and 4 w/v%) improved cell proliferation and adhesion compared to the ones at a higher concentration (8 w/v%) [109]. It was also concluded that such bioactive and biodegradable hydrogel systems could be a suitable option for *in vivo* use since they could increase tissue ingrowth as this is intimately linked with hydrogel degradation and impaired in non-degradable biomaterials [109].

In another recent study, the same group used these double-functionalized Alg hydrogels to develop microgel-based BioInks that were ionically linked with calcium chloride, and then photocrosslinked [112]. In brief, such microgel systems are composed of soft micro colloids [113] with unique rheological properties setting them apart from other polymeric systems. Indeed, microgel bioinks consisting of solid hydrogel microparticles offer a better alternative to conventional bioinks as they can flow easier through the extrusion needle during the printing phase, after which they can quickly stabilize themselves. Something intimately linked with a low flow behavior, good shear recovery, and better shear thinning properties compared to conventional

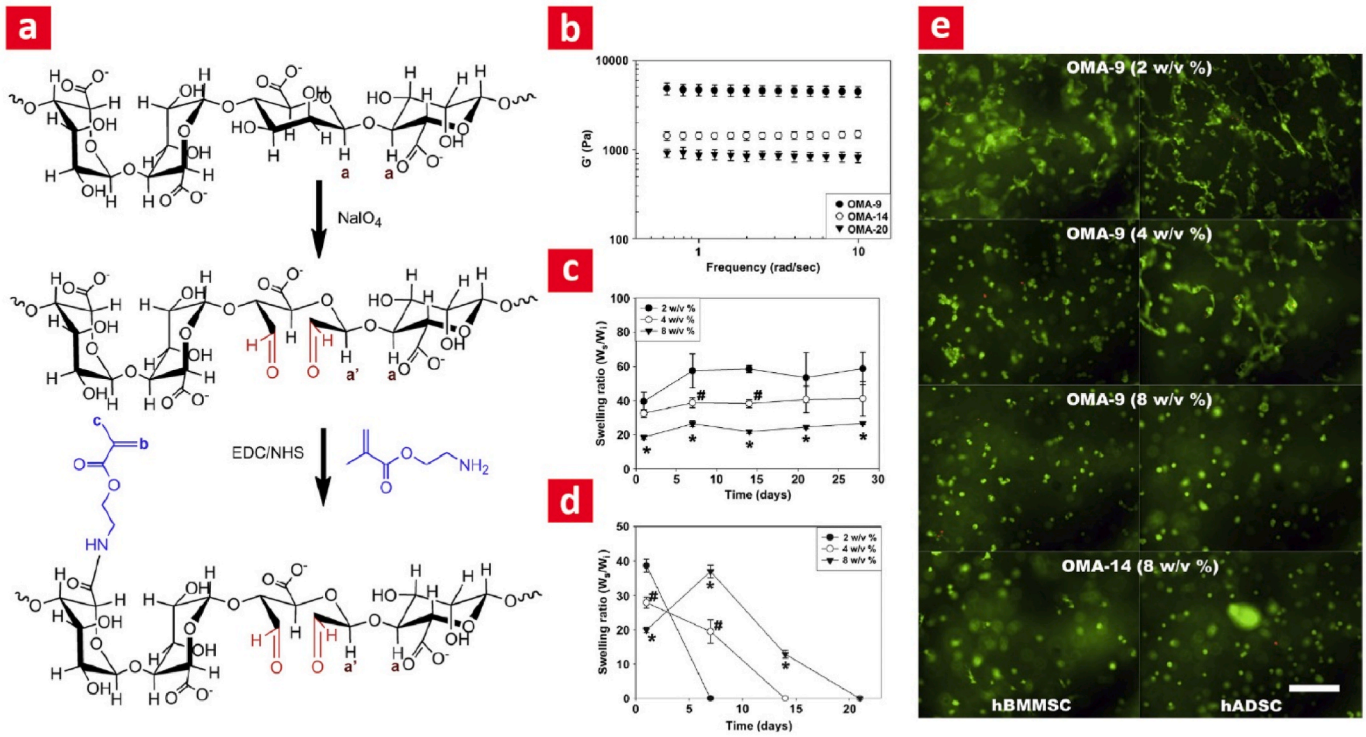

Fig. 5. Oxidized and methacrylated Alg (OMA) hydrogels – mechanical properties and biocompatibility. (A) The chemistry behind OMA synthesis is show here. (B) Mechanical properties as function of oxidation degree. (C) Swelling behavior of OMA-9 and (D) OMA-14 hydrogels. (E) Live-dead testing (**green** cells are alive and the **red** ones are dead) of human bone derived mesenchymal (hBMMSC's) and adipose derived mesenchymal stem cells (hADSC's). Adapted with permission [109]. Copyright 2012, Elsevier.

bioinks due to reversible and weak particle-particle interactions mediated by Van der Waals forces [114,115]. A follow-up study [25] concluded that 3D printed structures made with smaller Alg microgels lead to better prints, higher print stiffness, and yield strength. Therefore, smaller Alg microgels were considered more favorable bioinks than larger Alg microgels.

Ding et al., created hydrogels capable of altering their shape in a reversible and repeatable manner as needed. Their approach involves utilizing multilayered photocrosslinkable materials including oxidized, methacrylated alginate, and methacrylated gelatin. These materials enable the encapsulation of NIH3T3 and human mesenchymal stem cells within the hydrogel actuators, facilitating controlled and programmed movements. These cell-laden hydrogel actuators enable precise self-folding or user-directed folding into specific 3D structures under natural conditions. Their ability also allows for a partial imitation of intricate biological processes like branching morphogenesis [116].

A hydrogel system composed of jammed micro-flakes consisting of ionically cross-linked OMA, which are single components with varying sizes, was created as an innovative bioink for 4D bioprinting. This bioink exhibited favorable characteristics like shear-thinning and self-healing properties. It was directly printed into diverse 3D structures with high precision and accuracy, without the need for a support bath. Achieving shape changes over time (4D) was possible under natural conditions, and cell viability remained high following the establishment of a cross-linking gradient within the hydrogels. Notably, their approach was demonstrated by creating cartilage-like tissues within curved hydrogel bars and folded flower-like structures with four and six petals, serving as proof of concept [117].

Ding et al., developed a straightforward 4D bioprinting technique, that enabled the creation of a dynamic cell condensate-loaded bilayer structure. Their method generated scaffold-free cell condensates that gradually transformed into predetermined intricate shapes over time. Specifically, they fabricated bilayers loaded with cell condensates in specific shapes. The bilayers possess adjustable flexibility and microgel degradation, granting control over shape changes and the controlled release of reshaped cell condensates. Using this approach, sizable constructs filled with cell condensates and exhibiting various complex shapes were produced. As a demonstration, robust cartilage-like tissues in the form of a "C" letter and a helix were formed from hMSCs. Their method introduced a versatile concept for a 4D bioprinting platform, expected to enhance and streamline applications of 4D bioprinting based on cell condensation [118].

Along these lines, the same group has made several successful attempts at developing an OMA microgel bioink for 3D bioprinting [25, 119]. Here, they discovered that human bone marrow-derived mesenchymal stem cell (hMSC)-laden OMA microgels exhibited shear-yielding and thinning properties, making them suitable for 3D bioprinting, as shown in Fig. 6 [119]. Additionally, the bioprinted OMA bioink remained stable due to the fast mechanical recovery, something linked with the superior shear-thinning properties of the microgel ink. Finally, the authors demonstrated that hMSC-laden OMA microgels ink could be used for fabricating complex 3D tissue-like structures through extrusion printing while preserving the differentiation of hMSC into the chondrogenic and osteogenic pathways [119].

Even though the mechanical and hydration properties of OA hydrogels can change as a function of pH value, the responsiveness here is not so high compared to aminated stimuli-responsive polymers; why we envision the incorporation of dynamic imine bonds systems in such a system can increase the responsiveness substantially. Thus, by incorporating some aminated polymers into OA, stimuli-responsive OA-based bioinks suitable for 4D printing might be obtained. It is noteworthy that the structure of OA is composed of reactive aldehyde groups, which can be covalently bonded to the amine groups via a Schiff base reaction, resulting in the formation of stimuli-responsive Alg-based hydrogels [120]. The detailed mechanism here is based on the formation of carbinolamine due to the amine Nucleophilic attack on the carbonyl group,

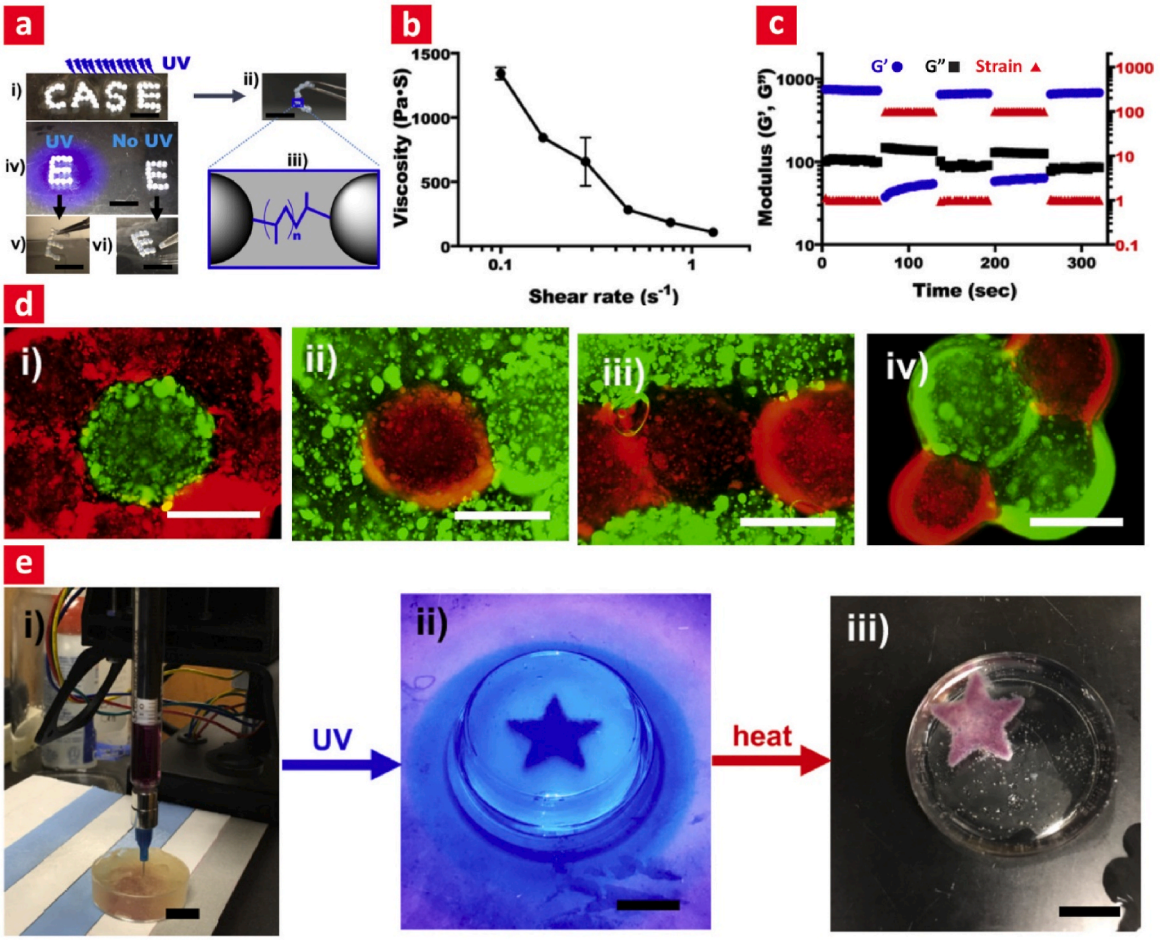

Fig. 6. OMA microgels for 3D printing of living tissues. (A) Photo-crosslinking of manually printed OMA migrogels. (B) Shear-thinning and (C) self-healing properties of OMA microgels. (D) Microgels were deposited into localized 3D structures containing either osteogenically (red) differentiated or chrondogenically (green) differentiated hMSC's. (E) Extrusion printing was used to deposit a star-shaped hMSC-laden construct, which was released as a free-standing structure by heat. Adapted with permission [119]. Copyright 2019, Elsevier.

followed by the removal of water, leading to the formation of imine bonds [16].

4.3.2. *Functionalization strategies*

Based on the discussion in section 2.6 we believe that the most obvious way to make stimuli-responsive Alg for 4D printing is to incorporate aminated systems into the ink due to their pH and thermo-responsiveness. Another alternative is to either graft amine groups onto its backbone or oxidize its backbone via aldehyde groups and incorporate amine-rich polymers to facilitate the formation of dynamic systems via imine bonds. Indeed; several studies have already shown how to aminate Alg via activation of its carboxylic groups through deprotonation followed by subsequent nucleophilic attack on the Alg backbone by the amine moiety [16,121–124]. For instance, Tan *et al.* [124] synthesized thermo-responsive aminated Alg-g-PNIPAAm hydrogels via grafting aminated Alg onto PNIPAAm-COOH through amide bonds. In brief, aminated Alg was synthesized by the addition of adipic dihydrazide, 1-ethyl-3-(3-dimethylaminopropyl) carbodiimide hydrochloride, and 1-hydroxybenzotriazole hydrate to Alg solution. The mixture was stirred at room temperature for 24h and finally dialyzed, and freeze-dried to obtain the purified aminated Alg. Next, to synthesize Alg-g-PNIPAAm copolymers, PNIPAAm-COOH was dissolved in water followed by incubation with 1-ethyl-3-(3-dimethylaminopropyl) carbodiimide hydrochloride for 48h at 4 °C. Subsequently the solution was mixed with an aminated Alg solution. Finally, the obtained aminated Alg-g-PNIPAAm was dissolved in PBS and kept for 15 min at 37 °C to form hydrogels. The *in vitro* degradation analysis demonstrated that modification with PNIPAAm enabled controlled degradation. The hydrogel encapsulation of human bone mesenchymal stem cells (hBMSCs) revealed that the Alg-g-PNIPAAm copolymer was non-toxic and effectively maintained the viability of the encapsulated cells. Overall, their thermo-sensitive nature of the AAlg-g-PNIPAAm copolymer presented appealing attributes, rendering it a promising candidate for delivering cells or pharmaceuticals in diverse tissue engineering applications [124].

Another potential avenue; is via imine bonds between aldehyde groups on the backbone of OA and amine-rich polymers such as GEL, collagen, or chitosan [123,125] through Schiff-base reactions. For instance, Chen et al. [125] fabricated dual stimuli-responsive (pH and smart redox) carboxymethyl chitosan (CMC)-OA-3,3′-dithiopropionic acid dihydrazide (DTP) hydrogels via triple dynamic bonds including acylhydrazone (O=NH–N), disulfide (S–S), and imine bonds. DTP is a crosslinker that has disulfide and hydrazide functional groups. In this regard, the aldehyde groups of OA were crosslinked to the imine bonds and acylhydrazone bonds of CMC and DTP, respectively. The prominent feature of hydrogels containing dynamic bonds is their environmental responsiveness. The CMC-OSA-DTP hydrogel possesses both dynamic disulfide bonds and acylhydrazone bonds, granting it the ability to respond to alterations in both redox conditions and pH through transitions between gel and sol states. Introduction of the reductant 1, 4-dithiothreitol (DTT) transformed the CMC-OSA-DTP hydrogel into a colloidal sol state by reducing initially formed disulfide bonds to free thiol groups. Conversely, the hydrogel regained its gel structure when an

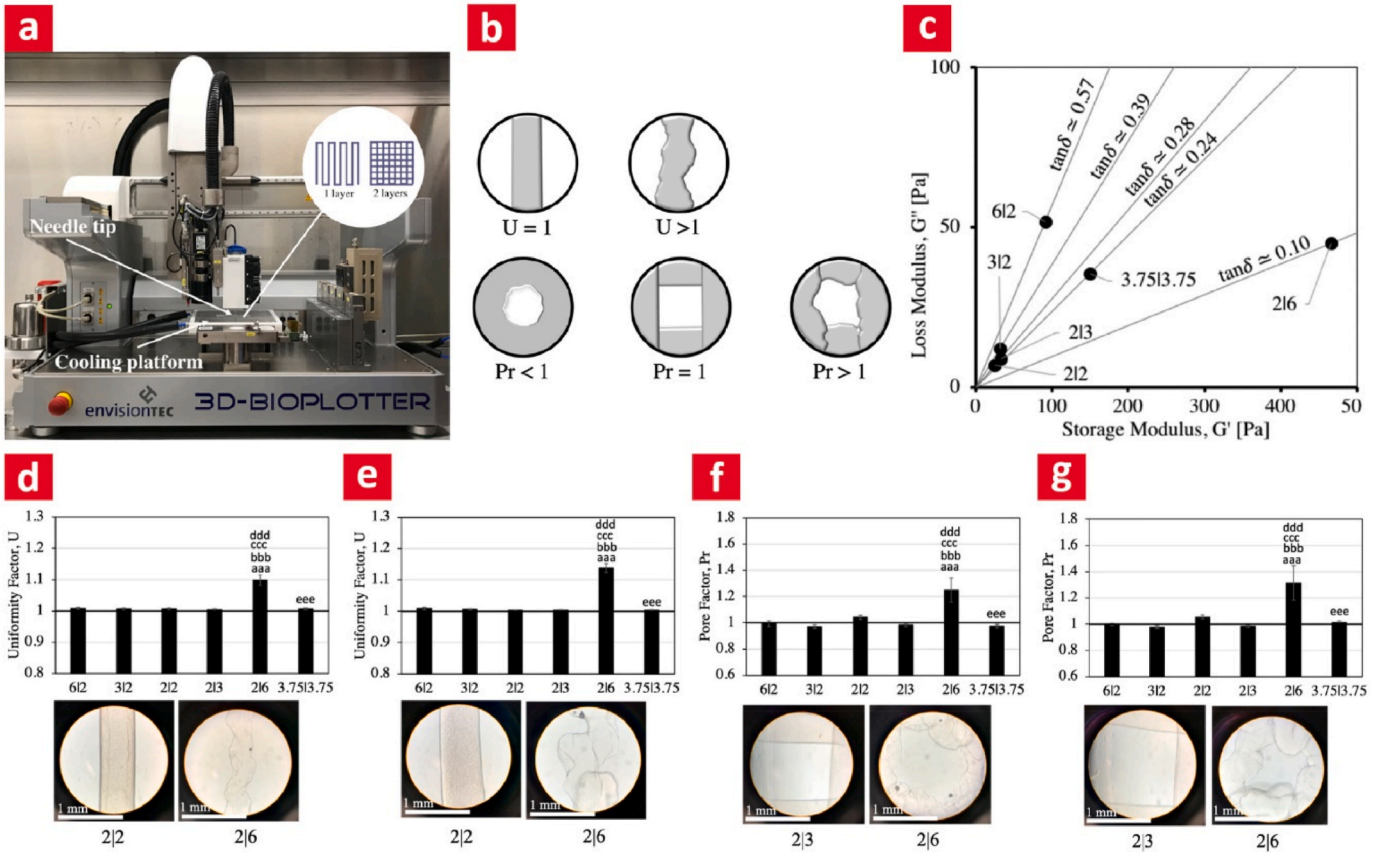

Fig. 7. 3D printing of OA-GEL hydrogels. (A) A schematic of the 3D printing setup used in the paper. (B) A description of how uniformity and pore factor were calculated. (C). Loss tangent modulus of the different tested combinations. The combinations are defined as X/Y = Alg/Gelatin and represent the weight ratio between alginate and gelatin. It is evident that the loss modulus decreased with increasing gelatin content. A small loss modulus represents a solid-like behavior, whereas a large one represents a more liquid-like behavior. (D–G) The uniformity and pore factor for different combinations are shown here. Adapted with permission [31]. Copyright 2019, American Chemical Society.

oxidizing agent like H_2O_2 was added. Alongside its redox sensitivity, the hydrogel also displayed reversible sol-gel transformations in response to changes in pH. Moreover, the results from mechanical assessments revealed a substantial enhancement in the mechanical strength of hydrogels due to the existence of dual cross-linking networks. The incorporation of both dynamic Schiff bases imine and acylhydrazone bonds facilitated the entanglement of polymer chains and mechanisms for stress dispersal, ultimately leading to enhanced elasticity as well as mechanical strength. Overall, they concluded that by fabricating CMC-OA-DTP hydrogels, their self-healing and injectability as well as their mechanical properties improved compared to CMC-OA and OA-DTP hydrogels. The compressive strength of the CMC-OSA-DTP hydrogel was remarkable due to the cooperative impact of dynamic bonds. Additionally, in some related works, PEG has been functionalized with DTP and as a result, acylhydrazone crosslinks can be formed between the aldehyde groups of oxidized Algs with the disulfide and hydrazide functional groups of (DTP) by the mechanism of Schiff base reactions. Moreover, the covalent acylhydrazone (O=NH–N) and disulfide (S–S) bonds can also lead to the formation of stimuli-responsive hydrogels [126]. For instance, Wang et al. [126] developed dual responsive Alg-based hydrogels (pH and redox) based on the Schiff reaction between the aldehyde groups of oxidized Algs and the amine groups of poly(ethylene glycol) PEG-DTP. The pH responsivity was obtained from the acylhydrazone bonds resulting from the reaction between the carboxyl groups of OA and amine groups of PEG-DTP. In this direction, the redox responsivity of Alg-based hydrogels was obtained from disulfide bonding in PEG-DTP [126]. The flexibility of the network was effectively enhanced by the presence of the soft macromolecular crosslinker (PEG-DTP), leading to a noticeable improvement in the mechanical performance of the PEG-DTP hydrogel. Additionally, the greater hydrophilicity of the crosslinker PEG-DTP significantly boosted the hydrophilic nature of the hydrogel's structure, resulting in enhanced pH sensitivity. The pH-adjustable gelation time facilitated good injectability of the PEG-DTP/ADA hydrogel. Its self-healing capability arose through the regeneration of dynamic acylhydrazone bonds after fracture, which reached 100% efficacy at room temperature. The biocompatibility of sodium alginate and PEG ensured that the PEG-DTP/ADA hydrogel was cytocompatible, as demonstrated through *in vitro* cytotoxicity assessment. Overall, they concluded that through the combination of PEG-DTP with OA hydrogel, the hydrophilicity, flexibility of PEG-DTP/OA hydrogel, and their mechanical properties improved compared to DTP-OA hydrogel. This Alg-based hydrogel, combining multi-stimuli responsiveness, injectability, and self-healing capacity, and therefore holds promise for applications in tissue engineering, controlled 3D cell culture as well as drug delivery. This methodology could thus be used to develop 4D printable Alg-inks that can be used to print tissue engineering constructs with improved mechanical properties and flexibility.

In summary, we can conclude that there are very few studies that deal directly with the preparation of Alg-based bioinks, which are suitable for 4D printing, limiting the development of 4D printed Alg structures. In most studies that have been done so far, 4D printable Alg hydrogels were mostly chemically modified with amine groups or prepared by the introduction of stimuli-responsive polymers such as PNIPAAm into the Alg matrix. We can thus conclude that maybe amino groups appear to be the most common denominator to this end. Indeed,

imine bonds can be achieved readily between carboxyl/aldehyde groups of Alg and amino groups from a secondary network, and it is pretty straightforward to include PNIPAAm into Alg as well; something that we will go into more depth within section 4.2.3. However, PNIPAAm has some limitations, including its non-biodegradable nature, lack of bio-resorbability as a polymer, and limited biocompatibility, limiting its applications in tissue engineering and clinical applications [127].

4.3.3. 4D printable Alg inks

A number of strategies involving Alg methacrylation [128,129] or the inclusion of polydopamine (PDA) [129], methylcellulose [130], and PNIPAAmm [131–133] can also give rise to 4D printable inks. Among the stimuli-responsive polymers that have already been successfully 4D printed, PNIPAAm is the most frequently applied due to its excellent thermo-responsiveness. We will thus focus on Alg-PNIPAAm composites in this section.

In simple terms, the structure of PNIPAAm is made up of two groups, isopropyl and amide groups, which are hydrophobic and hydrophilic, respectively [134]. The phase separation mechanism of PNIPAAm is based on the release of water molecules attached to its isopropyl groups above the LCST point. This then leads to increased hydrophobic interactions between the isopropyl groups and a collapsed state [105]. Interestingly, Alg can be grafted onto amino-functionalized PNIPAAm (PNIPAAm-NH_2) using 1-ethyl-3-(3-dimethylaminopropyl) carbodiimide hydrochloride and N-hydroxybenzotriazole as condensing and coupling agents, respectively to develop thermo-responsive hydrogels.

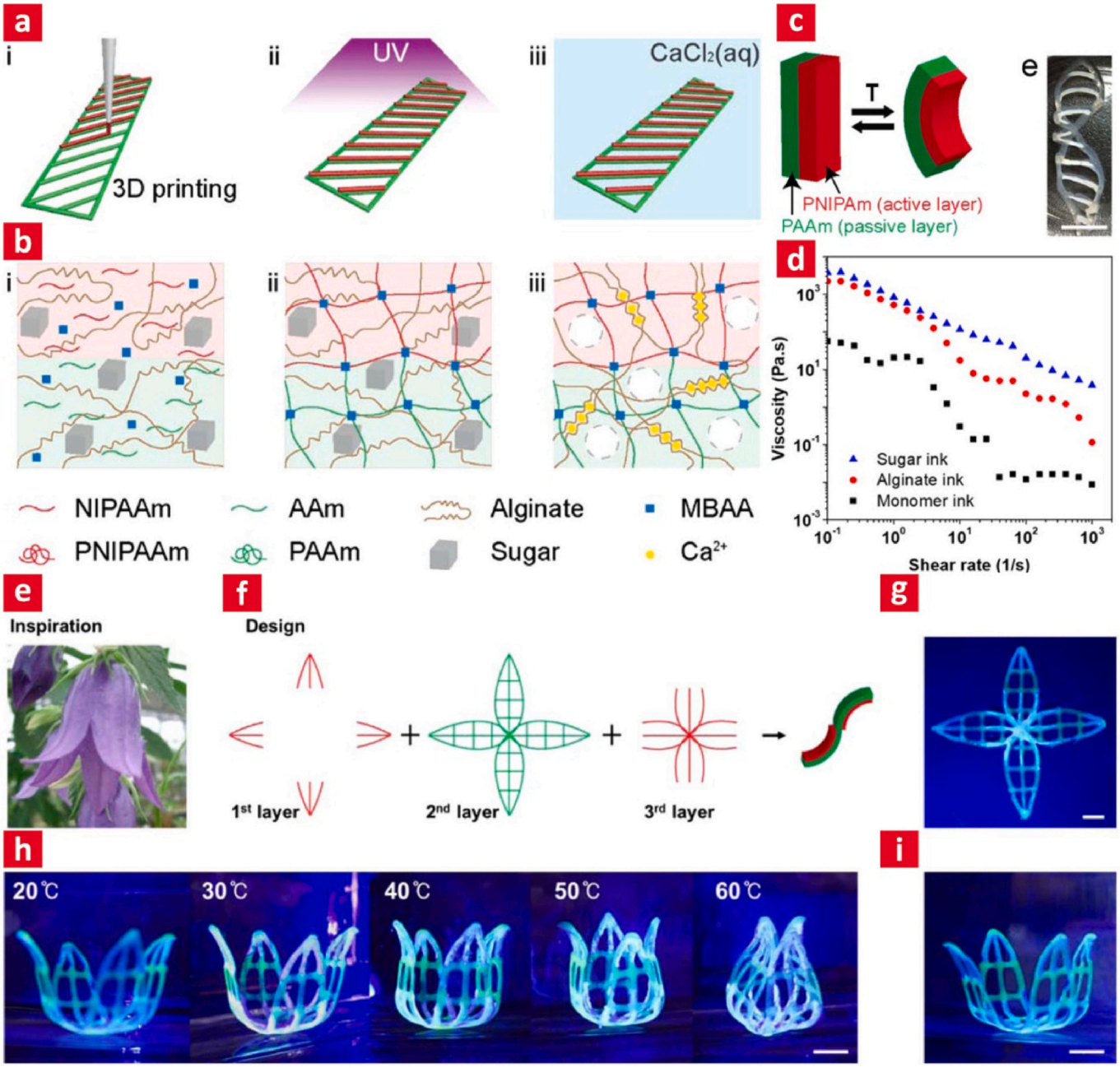

Fig. 8. 4D printable Alg inks based on PNIPAAm. (A, C) Schematics showing the concepts behind the 4D printing approach used in the paper. (B) Schematic showning the chemistry behind the employed materials for 4D printing of a flower-like structure. (E–G) Inspiration and design. (H) As the temperature increased the printed flower-like structure gradually took shape. (I) Recovered shape after re-cooling to room temperature. Adapted with permission [133]. Copyright 2020, Macmillan Publishers Ltd.

Here, the grafted copolymers are formed by the amide coupling reaction between the free amine group present in the amino-PNIPAAm and carboxylate group present in the sodium Alg [135]. Similarly, PNIPAAm-NH_2 can also be grafted to the carboxylate groups of Alg via *N, N'*-dicyclohexylcarbodiimide (DCC)-mediated amidation using *N*-hydroxysuccinimide (NHS) [136,137]. In another approach, a non-covalently linked Alg-PNIPAAm network was generated via electrostatic interaction between the positively charged amine group in the PNIPAAm-NH_2 and negatively charged carboxylate groups present in the Alg backbone [137].

Such, temperature-responsive inks based on Alg and PNIPAAm can be used for 4D printing. In this direction, Bakarich et al. [132] developed a 4D printed actuator based on Alg-PNIPAAm, which could be actuated by heating/cooling in the range of 20–60 °C. The hydrogels were fabricated through extrusion 3D printing coupled with a UV curing system. In this regard, the Alg-PNIPAAm hydrogel inks were prepared by mixing Alg with PNIPAAm solution. The bioinks were bioprinted and then cured with UV light for 200 s. Finally, the bioprinted hydrogels were soaked in $CaCl_2$ solution for 3 days to obtain complete crosslinking. Along these lines, they observed that as the NIPAm concentration increased from 10 to 20 w/v%, the swelling degree increased below LCST. On the other hand, with increasing NIPAAm concentration above LCST, the swelling degree decreased due to its higher shrinkage capacity. Moreover, by cooling the Alg/PNIPAAm hydrogels from 60 to 20 °C, the expansion increased from 41% to 49%.

In a similar study, Ko et al. [133] fabricated a bilayer structure, using two hydrogel compositions including Alg/PAAm and Alg/PNIPAAm (Fig. 8a-c). The first layer as the passive layer was printed from sugar/PAAm/Alg ink, and the second layer as the active layer was printed from sugar/PNIPAAm/Alg ink. Afterwards, the two layers were exposed to UV light for 1–5 min to facilitate crosslinking. Subsequently, the polymerized structure was immersed in 10% (w/v) calcium chloride solution, resulting in simultaneous crosslinking of Alg chains in both layers. The results demonstrated that the addition of Alg to the hydrogel composition resulted in an increased viscosity of the ink (>4500% at 10^{-1} s^{-1}) and a strong shear-thinning behavior, as assessed through shear viscosity measurements (Fig. 8d). Additionally, a double-crosslinked network hydrogel was created in the printed structure by ionic crosslinking of the structure with calcium chloride. Moreover, the sugar was added to the ink as a pore-generator to improve printability by increasing the viscoelastic properties of the ink as well as creating macropores in the structure, leading to stimuli responsiveness and thereby 4D printability (Fig. 8b). They fabricated a printed configuration imitating the form and motion of a bellflower (Fig. 8e). The printing strategy entailed three distinct layers (Fig. 8f) designed to replicate the S-shaped curvatures of the bellflower's petals, as the structure curved towards the PNIPAAm layers. Subsequently, the resultant printed design (Fig. 4g) was submerged in water, instigating swelling and shape morphing as a response to temperature fluctuations. Finally, the printed hydrogels demonstrated a temperature-responsive behavior, which was achieved by fine-tuning it's swelling and shrinking properties. In this direction, the hydrogels were swollen in water at 25 °C for at least 24 h and then immersed in warm water at 50 °C. It was found that the bilayer structure shrunk and bent at 50 °C due to the presence of temperature-responsive PNIPAAm and then recovered after cooling to 20 °C as shown in Fig. 8 h [133]. Nevertheless, the process of shape transformation displayed irregularities and variations during the cooling-driven recovery phase. In the majority of instances, the structure entirely restored its initial configuration, a transformation occurring at 20 °C over a span of 15 min (Fig. 8i).

A number of recent studies have also used methacrylated Alg for designing 4D inks. The reason is that methacrylated Alg has carboxylic groups in its structure, which shows stimuli responsiveness to ions and can thus display shape change upon swelling. For instance, Constante et al. [129] fabricated a 4D printed self-foldable by combining methacrylated Alg with melt electrowritten polycaprolactone (PCL) fibers. In brief, methacrylated Alg solution with photoinitiator was printed and then crosslinked with UV light for 15 min and finally dried. Subsequently, PCL fibers were added to the cross-linked methacrylated Alg layer through meltelectrowriting and then the whole system was cross-linked with UV light. Notably, the crosslinked methacrylated Alg layer displayed responsiveness to calcium ions and exhibited rolling upon swelling, thereby creating scroll-like tubes. Because calcium ions acted as a stimulus to induce the shape transformation and contribute to accurately controlling the folding process. Similarly, the results demonstrated the shape-morphing behavior of the fabricated bilayer hydrogels. It was for instance found that bilayers were rolled into tubes in a calcium-free aqueous environment. The authors concluded that the introduction of calcium ions caused the bilayer structure to be unfolded and the addition of ethylenediaminetetraacetic acid (EDTA) led to the folding of the pristine bilayer structure [129]. Moreover, myoblast behavior was studied on these printed shape-changing bilayers. The myoblasts were highly viable and proliferated on the methacrylated Alg film as well as the bilayer film. In addition, PCL fibers enabled extremely high levels of cell orientation, which was not accomplished with methacrylated Alg films alone. Cell assays revealed that the metabolic rate was higher on bilayer films compared to methacrylated Alg films. Both methacrylated Alg films and bilayer films showed similar viability via live/dead assay. Staining of the actin filament and cell nuclei revealed the alignment of the cells. In this regard, 65% of the cells seeded over the bilayer scaffolds showed strong alignment on day 1 as a result of the melt-electrowritten PCL fibers. Conversely, the cells seeded over methacrylated Alg did not align. Cell alignment on the bilayer decreased to 60 and 58%, respectively, after 3 and 7 days of culture due to the agglomeration of cells [129].

In another approach, Kirillova et al. [128] developed a 3D-printed self-foldable tube (Fig. 9a). They could fold and unfold in response to calcium ions due to the calcium-dependent swelling behavior of the methacrylated Alg structures. Methacrylated Alg was printed onto polystyrene or glass surfaces and then the printed hydrogels were covalently crosslinked with green light and dried. Afterwards, the crosslinked hydrogels were immersed in water, cell culture media, or PBS, swelled, and folded into tubes, resulting in the shape transformation of the hydrogels in a few seconds due to the presence of calcium ions as observed in Fig. 9 b [128]. In more detail, the photo-crosslinked hydrogels indicated a reversible behavior of folding and unfolding upon immersion in 0.1 M calcium chloride as this was linked to the absence and presence of calcium ions, respectively. Importantly, this shape-morphing behavior was ascribed to the presence of carboxylic groups in the hydrogel structure. Moreover, these tubes were stable in water for at least six months [128]. Cells encapsulated inside the tubes also displayed high viability as evident from Fig. 9c-d. Moreover, the cell-laden methacrylated Alg hydrogels exhibited reversible shape changes when exposed to Ca^{2+} ions. They later used a suspension of D1 cells (mouse bone marrow stromal cells) in a solution of 3% methacrylated Alg. To this end, a red fluorescent marker was applied to the cells before the bioprinting experiment so that they could be visualized within the folded hydrogels after printing. The results indicated that the cells were evenly distributed throughout the hydrogels, which suggests that the cells had been successfully mixed with the printable methacrylated Alg solution. Importantly, despite the high cell density the films maintained their folded structure, and the cells were uniformly distributed within hydrogel-based tubes. It was observed that the 4D-printed tubes were capable of keeping the cells alive for at least 7 days without any loss of viability [128].

In a similar study, Lee et al., tuned the spatial patterning of the two biomaterials (OMA/GelMA) with different swelling ratios to obtain a controllable geometric change of the printed construct over time by creating complex 4D configurations featuring dense cell populations, capable of orchestrated and controlled changes in shape. These alterations were guided by the precise arrangement of biodegradable OMA and GelMA materials, each with distinct swelling behaviors. By

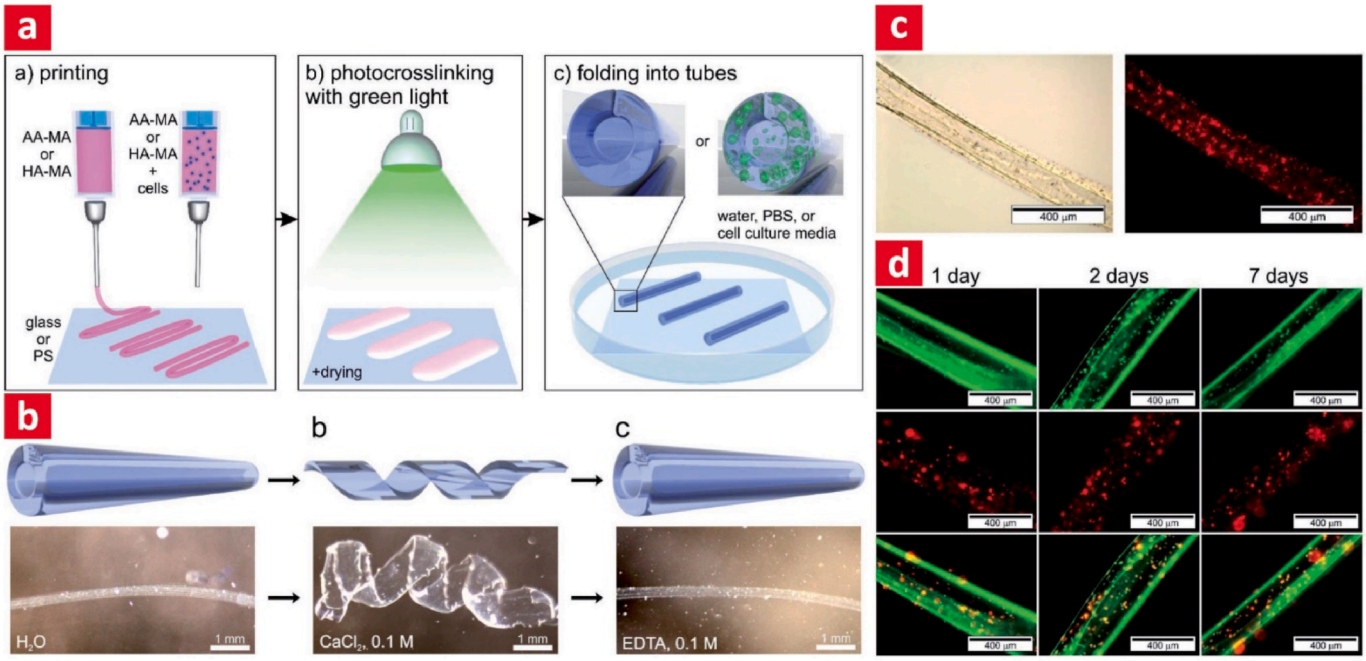

Fig. 9. 4D printable Alg inks based on methacrylated alginate (AA-MA) and methacrylated hyaluronic acid (HA-MA). (A–B) Schematics showing the concepts behind the 4D printing approach of the vascular-like tubes. (C) Cell-laden dried tubes. (D) Images of cell-laden tubes after 1, 2 and 7 days of culture. Live cells are stained green and (Live + dead) cells are red. Adapted with permission [128]. Copyright 2017, Wiley-VCH.

employing a bilayered OMA/GelMA hydrogel model, they showed that a higher degree of OMA oxidation led to increased degradation and swelling, something which in turn resulted in more pronounced modifications in geometric structure. Various variables, including macromer ratios, layer thickness, cell concentration, and photolithography patterns, were finely tuned to exert precise control over the ultimate form of the 4D structure. Furthermore, Fibroblasts and human adipose-derived stem cells (ASCs) were enclosed within the 4D structures at a high density of 1.0×10^8 cells mL^{-1}. The orchestrated changes in shape harmonized with the differentiation process of ASCs, as they transformed into chondrogenic and osteogenic lineages. The incorporation of densely packed cells into OMA and GelMA using bioprinting enabled the creation of more intricate structures, exhibiting well-defined 4D transformations. This strategy effectively facilitated typical cellular functions, allowing differentiation into osteogenic and chondrogenic lineages with minimal effect on cell viability [138].

Altogether, stimuli-responsive materials hold significant potential for various applications in the field of tissue engineering such as drug delivery systems [139], wound healing, biosensors, vascular tissue engineering, etc. [140,141]. For instance, photo-crosslinked hydrogels such as Methacrylated alginate hold promise in the field of tissue engineering as a responsive material sensitive to external cues. This responsiveness is attributed to the carboxylic groups within its composition, allowing it to react to ions and exhibit shape-morphing behavior when subjected to swelling. Employing either UV-induced crosslinking or introducing EDTA and calcium chloride are suitable techniques for inducing sensitivity to calcium ions, leading to the material demonstrating a response such as folding and unfolding upon swelling. The size of the tubes can be finely adjusted by altering the concentration of calcium ions, which also impacts the swelling characteristics of the Alg hydrogel. Gradually increasing the calcium ion concentration led to a reduction in swelling, causing the tubes to unfold and expand in diameter. Modulating the concentration of Ca^{2+} ions in this way serves as a stimulus to initiate controlled shape changes. Introducing EDTA permits reversible unfolding. The mechanical and swelling properties of the hydrogel layers are influenced by both the concentration of the photoinitiator and the duration of cross-linking. It was observed that higher levels of IRG2959 and longer cross-linking times resulted in greater elastic modulus in the formed hydrogel sheets [129]. Hence, the duration of UV exposure, utilization of biocompatible solvents, and the concentration of EDTA/CaCl2 are crucial elements that can impact the material's responsiveness, facilitating the creation of a stimuli-sensitive material well-suited for applications in tissue engineering. In summary, the wide-ranging and varied potential uses of stimuli-responsive materials in tissue engineering provide avenues to develop enhanced and flexible approaches for restoring, regenerating, and repairing tissues with greater efficacy.

Overall, stimuli-responsive Alg bioinks can be prepared from a wide range of polymers as we discussed previously. They were mostly chemically modified with amine groups or prepared by the introduction of a stimuli-responsive polymer such as PNIPAAm into the Alg backbones to make them either pH or thermo-responsive. However, PNIPAAm can be considered the most effective option considering its promising benefits. Despite the reviewed studies here in terms of 4D printable PNIPAAm-functionalized Alg ink – the studies are few in number and the area of 4D printable Alg ink is still uncharted territory for biomedical engineers. We can therefore conclude that there is still a gap in the development of dynamic Alg bioinks and the mechanism of how we can turn them into 4D printable bioinks is still not fully elucidated**.** To overcome this, we propose OA as a more effective method than amine bonding which can be applied in the future. Because OA is stimuli-responsive and highly printable, it is worthwhile trying them out for 4D printing. The advantage of using OA is its simple preparation without the need for toxic reagents and high temperatures. Moreover, it is highly printable and easy to fine-tune in many ways in addition to being more scalable and easier to work with than by including additional amine-rich polymers into the system. For these reasons, we anticipate that modification of Alg with amino-groups along the Alg backbone or by using oxidized Algs, might be more suitable in this regard. These approaches could indeed facilitate stimuli-responsive Alg bioinks suited for the 4D printing of smart materials with multifunctional properties in the near future. Overall, they could lead to the development of smart Alg-based bioinks for the fabrication of 4D printed structures that could be suitable for various tissue engineering

applications. However, more studies need to be carried out in this direction, and one of the important gaps in the field is that future studies could target.

5. Possible future applications of 4D-printed alginate constructs

In this section, we review possible methods to make various cell-laden Alg inks for 4D printing applications with a special focus on generating vascularized tissue engineering constructs using dynamic materials that can self-fold into hollow blood-vessel-like tubes based on chemical modification (methacrylated Alg) or by including a stimuli-responsive polymer such as PDA alongside its network. Moreover, the behavior of cells within these Alg hydrogels will be reviewed as well. We will not go in depth with 3D bioprinted Alg constructs, since a lot has been written about this topic, but will instead refer the interested reader to several excellent reviews [36,51–53,66,71].

5.1. 4D printed cell-laden alginate-based constructs

With 4D printing, one can generate complex and biomimetic 3D microstructures by using dynamic materials that can self-fold into complicated geometries. The initial step in this regard is based on developing a micro-patterned sheet that later can be assembled into higher-order structures. Photolithography, soft lithography, stereolithography, and extrusion-based printing are the most common ways to manufacture time-dependent and dynamic sheets for 4D printing. However, these strategies often require a considerable production time, along with expensive machinery and thorough user training. Conversely, inkjet printing presents a mask-free and readily available manufacturing method, enabling swift micro-patterning as well as

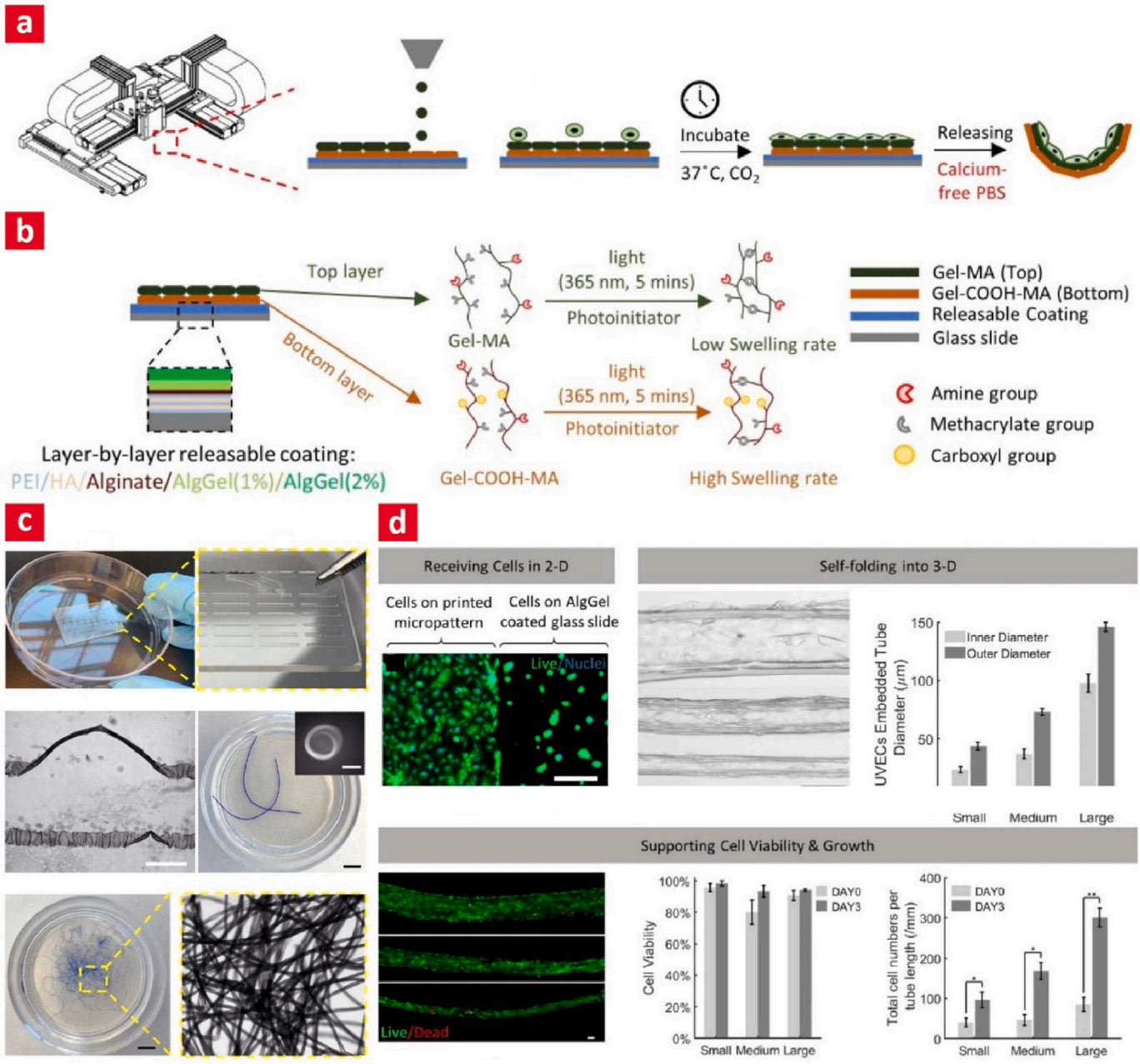

Fig. 10. 4D printing of lumen-like tissues via modified alginate and gelatin-based hydrogels. (A) Schematic of the 4D printing setup. (B) Schematic of the materials used and the chemistries behind them. (C) Photographic images showing the self-folded constructs. (D) Studies demonstrating that the 4D printed constructs can support cell viability and growth. Adapted with permission [142]. Copyright 2020, IOP Publishing.

prototyping. In a recent study [142], this pathway was used for the 4D printing of vascularized tissue engineering constructs. The authors specifically created a GelMA and Gel COOH-MA blend ink, which was light crosslinkable. Alg-Gel was used as a sacrificial coating on the glass substrate, which allowed a controlled release of micropatterns. It helped to improve its adhesion to the 4D-printed micropatterns and prevented the micropatterns from detachment and self-folding in the presence of culture medium and living cells. They specifically printed rectangular 2D microstructures via inject printing and then controlled their swelling behavior by using light crosslinking (Fig. 10 a.b). Over time the cell-laden rectangular structures self-folded into long microtubular scaffolds Fig. 10 c. They then seeded Human umbilical vein endothelial cells (HUVECs) onto the as-printed rectangular structures. The viability of cells within the microtubes where then evaluated on day 0 and day 3 and was above 90% for all microtube diameters at day 3. After day 3 an increased density was observed for all combinations, however, the cell density was significantly different within the medium (168.4 cells mm^{-1}) and large microtubes (301.3 cells mm^{-1}) compared to the smaller tubes (96.8 cells mm^{-1}) as shown in Fig. 10 d [142]. The contraction of the cytoskeleton of proliferating cells on a 3D scaffold could gradually distort the scaffold, which is undesirable for tissue engineering (Fig. 10d). The inner diameters of the HUVEC-encapsulating microtubes were therefore measured during three days of cell culture to investigate this effect. These results demonstrated that the microtubes have enough mechanical strength to sustain their 3D structures in the presence of proliferating cells.

Other studies have focused on Alg polymers functionalized with methacrylate groups to fabricate stimuli-responsive polymers. For instance, Constante et al. [129] created anisotropic scaffolds with a scroll-like configuration to facilitate the growth of oriented muscle tissue by combining extrusion printing of methacrylated Alg and melt-electrowriting of PCL fibers. Notably, the photo-cross-linked 3D printed Alg sheets rolled into tubes when swollen in the presence of calcium ions, and thereby formed scroll-like tubes. Myoblast behavior was studied on these printed shape-changing bilayers. The myoblasts were highly viable and proliferated on the methacrylated Alg film as well as the bilayer film. In addition, PCL fibers enabled extremely high levels of cell orientation, which was not accomplished with methacrylated Alg films alone. Cell assays revealed that the metabolic rate was higher on bilayer films compared to methacrylated Alg films. Both methacrylated Alg films and bilayer films showed similar viability via live/dead assay. Staining of the actin filament and cell nuclei revealed the alignment of the cells. In this regard, 65% of the cells seeded over the bilayer scaffolds showed strong alignment on day 1 as a result of the melt-electrowritten PCL fibers. Conversely, the cells seeded over methacrylated Alg did not align. Cell alignment on the bilayer decreased to 60 and 58%, respectively, after 3 and 7 days of culture due to the agglomeration of cells. In a similar study, Kirillova et al. [128] created hollow self-folding methacrylated Alg hydrogel tubes. Here they were able to precisely control the diameters and architectures of the tubes by using a 4D biofabrication technique. For instance, the cell-laden methacrylated Alg hydrogels exhibited reversible shape changes when exposed to Ca^{2+} ions. They later used a suspension of D1 cells (mouse bone marrow stromal cells) in a solution of 3% methacrylated Alg. A red fluorescent marker was applied to the cells before the bioprinting experiment so that they could be visualized within the folded hydrogels after printing. The results indicated that the cells were evenly distributed throughout the hydrogels, which suggests that the cells had been successfully mixed with the printable methacrylated Alg solution. Importantly, despite the high cell density the films maintained their folded structure, and the cells were uniformly distributed within hydrogel-based tubes. It was observed that the 4D printed tubes were capable of keeping the cells alive for at least 7 days without any loss of viability.

Luo et al. [3] fabricated 4D-printed near-infrared (NIR)-triggered shape morphing hydrogels for vascularized tissue engineering constructs. In this regard, they printed biphasic hydrogels consisting of cell-laden Alg/PDA inks and Alg/GEL methacryloyl (GelMA) bioinks with controlled curved structures (Fig. 11a). Next, the hydrogels were photo-crosslinked with UV light, after which they injected calcium chloride solution on the surface of the hydrogels to crosslink the Alg structure. Subsequently, the rest of the calcium chloride solution was eliminated, and the hydrogels were exposed to laser irradiation. Finally, the crosslinked hydrogels were maintained over 24 h at room temperature for dehydration-induced shape morphing. It was found that the printed hydrogels demonstrated shape-folding behavior during dehydration since their structures were transformed from lamellar to saddle-like structures. The results demonstrated that the shape-morphing behavior can be adjusted by regulating the irradiation time and laser power. Rapid shape morphing was obtained with higher laser power since it raised the temperature and caused a faster dehydration rate as can be seen in Fig. 11 b [3]. Notably, it was found that the deformed hydrogels could recover to their initial structures by immersion in EDTA solution, as they can remove the calcium ions as a crosslinking agent Fig. 11 c [3]. Moreover, due to the ability to control the shape of the scaffolds by using NIR irradiation, the non-deforming parts were used for cell encapsulation. To this end, human embryonic kidney cells were added to composite inks, and cell-laden scaffolds were made. The cell-laden scaffold subsequently transformed into a saddle-like via NIR structure with high cell viability of about 80% after 14 days as shown in Fig. 11 d [3]. It was found that cells survived well in scaffolds before and after NIR-induced shape morphing. The authors therefore concluded that these curved cell-laden structures can be used as cardiac patches or scaffolds for skin and cartilage tissue regeneration applications.

6. Conclusion

Today when you bioprint tissue constructs they are static, and thus do not really have any added value for being used inside the body. They are amenable for building tissues for disease modeling or even high-throughput drug screening – but beyond that, they are pretty useless. We thus need to move beyond 3D bioprinting to allow the industry to gain the momentum it truly deserves. This could ultimately generate a paradigm shift in the healthcare industry. With 4D printing, the story becomes entirely different. The constructs are native-like and adaptable and can respond to physiological stimuli to change their architecture and functionality when needed. Even still both 4D and 3D Biopriting are typically based on extrusion printing. Decades of experiences along these lines have made it clear that 3D bioprinting technologies based on extrusion are only appropriate for entry-level research. The road toward their usage in realistic applications is still farfetched. Emerging technologies based on magnetic levitation, and acoustic and electric self-assembly of bioinks in predesigned nano and microshapes might change this, and even disrupt the industry as we know it. After all, how thin materials can you extrude through a needle without damaging cells? And how big constructs can you build before material spillover and pattern loss becomes a problem?

Due to the lack of research in the field of stimuli-responsive Alg hydrogels, further studies need to be done to overcome limitations such as the inability of Alg to respond to stimuli due to the lack of proper chemical groups in its structure, its brittleness and the lack of cell-adhesive motifs. By developing smart Alg bioinks through various functionalization strategies, researchers may be able to fabricate 4D printed structures for tissue engineering applications. To this end, various Alg hydrogels with shape-morphing properties and self-foldable structures have been identified. They have displayed stimulate-responsiveness, biocompatibility, and good support for cellular functions making them suitable for a wide range of applications. Additionally, several routes have been explored to modify them even more via smart chemistry as well as nanomaterial reinforcement. For instance, the conjugation with PNIPAAm and other functional groups has to lead to

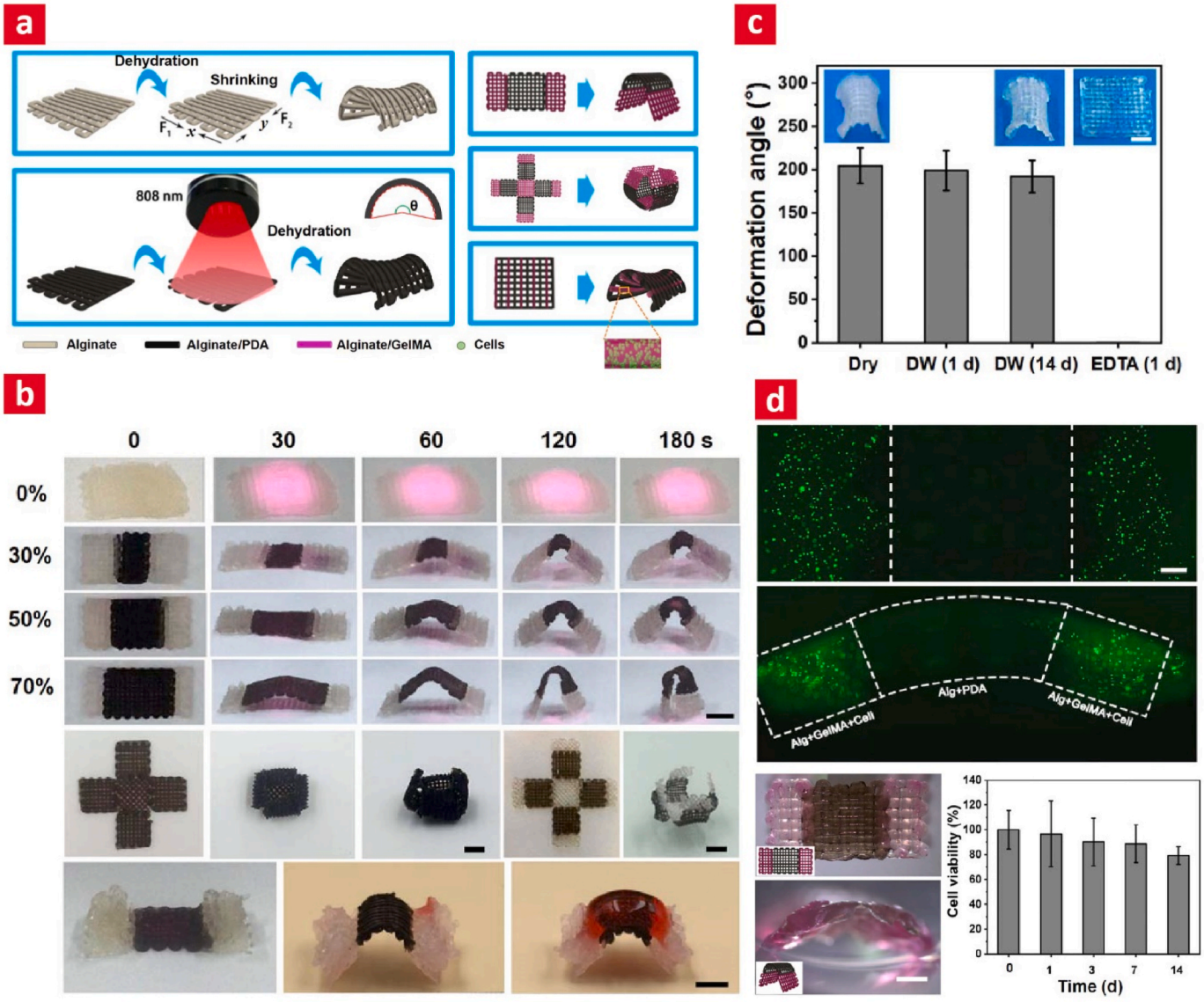

Fig. 11. 4D printable Alg inks based on alginate and GelMA. (A) Schematics showing the concepts behind the 4D printing approach. (B) Constructs with varying alginate/PDA content were printed, and then exposed to near-infrared light to facilitate shape changes. (C) Shape-recovery of the folded constructs in deionized water (DW) and EDTA are shown here. (D) Images of cell-laden constructs demonstrating good biocompatibility of the 4D printed constructs even after 7 days of culture. Adapted with permission [3]. Copyright 2019, IOP Publishing.

desirable stimuli responsiveness in Alg inks making them useful for a wide range of 4D printing applications. For instance, 4D bioprinting of Alg hydrogels has enabled good vascularization and the introduction of biological functions in the engineered tissues, allowing the host tissues to be integrated better with it. Until now, however, the focus has been on vascularization, therefore more studies are needed in this direction for identifying the gaps that can enable adaptable Alg bioinks to be used in other applications as well. Overall, due to the numerous favorable characteristics exhibited by Alg and the possibilities presented by 4D printing, their extensive utilization can be envisioned in the realm of tissue engineering, encompassing various biomedical applications like drug delivery, flexible robotics, biosensors, and bioelectronic devices.

Declaration of competing interest

The authors declare that they have no known competing financial interests or personal relationships that could have appeared to influence the work reported in this paper.

Data availability

Data will be made available on request.

Acknowledgements

A.D.-P. would like to acknowledge the VIDI research programme with project number R0004387, which is (partly) financed by The Netherlands Organisation for Scientific Research (NWO). This work has also received funding from the European Union's Horizon 2020 research and innovation programme under grant agreement no. 951747.

References

[1] D.F. Williams, Challenges with the development of biomaterials for sustainable tissue engineering, Front. Bioeng. Biotechnol. 7 (2019) 127.
[2] H. Wobma, G. Vunjak-Novakovic, Tissue engineering and regenerative medicine 2015: a year in review, Tissue Eng. B Rev. 22 (2) (2016) 101–113.

[3] Y. Luo, X. Lin, B. Chen, X. Wei, Cell-laden four-dimensional bioprinting using near-infrared-triggered shape-morphing alginate/polydopamine bioinks, Biofabrication 11 (4) (2019), 045019.

[4] S. Mohanty, M. Alm, M. Hemmingsen, A. Dolatshahi-Pirouz, J. Trifol, P. Thomsen, M. Dufva, A. Wolff, J. Emnéus, 3D printed silicone–hydrogel scaffold with enhanced physicochemical properties, Biomacromolecules 17 (4) (2016) 1321–1329.

[5] M. Mehrali, A. Thakur, C.P. Pennisi, S. Talebian, A. Arpanaei, M. Nikkhah, A. Dolatshahi-Pirouz, Nanoreinforced hydrogels for tissue engineering: biomaterials that are compatible with load-bearing and electroactive tissues, Adv. Mater. 29 (8) (2017), 1603612.

[6] S. Talebian, M. Mehrali, N. Taebnia, C.P. Pennisi, F.B. Kadumudi, J. Foroughi, M. Hasany, M. Nikkhah, M. Akbari, G. Orive, Self-healing hydrogels: the next paradigm shift in tissue engineering? Adv. Sci. 6 (16) (2019), 1801664.

[7] F. Abasalizadeh, S.V. Moghaddam, E. Alizadeh, E. Kashani, S.M.B. Fazljou, M. Torbati, A. Akbarzadeh, Alginate-based hydrogels as drug delivery vehicles in cancer treatment and their applications in wound dressing and 3D bioprinting, J. Biol. Eng. 14 (1) (2020) 1–22.

[8] A. Memic, A. Navaei, B. Mirani, J.A.V. Cordova, M. Aldhahri, A. Dolatshahi-Pirouz, M. Akbari, M. Nikkhah, Bioprinting technologies for disease modeling, Biotechnol. Lett. 39 (9) (2017) 1279–1290.

[9] M. Rafiee, R.D. Farahani, D. Therriault, Multi-material 3D and 4D printing: a survey, Adv. Sci. 7 (12) (2020), 1902307.

[10] E. Sodupe-Ortega, A. Sanz-Garcia, A. Pernia-Espinoza, C. Escobedo-Lucea, Accurate calibration in multi-material 3D bioprinting for tissue engineering, Materials 11 (8) (2018) 1402.

[11] M.H. Ali, N. Mir-Nasiri, W.L. Ko, Multi-nozzle extrusion system for 3D printer and its control mechanism, Int. J. Adv. Des. Manuf. Technol. 86 (2016) 999–1010.

[12] L. Ionov, 4D biofabrication: materials, methods, and applications, Adv. Healthcare Mater. 7 (17) (2018), 1800412.

[13] D.T. Butcher, T. Alliston, V.M. Weaver, A tense situation: forcing tumour progression, Nat. Rev. Cancer 9 (2) (2009) 108–122.

[14] I.P.S. Fernando, W. Lee, E.J. Han, G. Ahn, Alginate-based nanomaterials: fabrication techniques, properties, and applications, Chem. Eng. J. 391 (2020), 123823.

[15] M. Marchand, E.K. Anderson, S.M. Phadnis, M.T. Longaker, J.P. Cooke, B. Chen, R.A. Reijo Pera, Concurrent Generation of Functional Smooth Muscle and Endothelial Cells via a Vascular Progenitor, Oxford University Press, 2014, pp. 91–97.

[16] S.N. Pawar, K.J. Edgar, Alginate derivatization: a review of chemistry, properties and applications, Biomaterials 33 (11) (2012) 3279–3305.

[17] M. Szekalska, A. Puciłowska, E. Szymańska, P. Ciosek, K. Winnicka, Alginate: current use and future perspectives in pharmaceutical and biomedical applications, International Journal of Polymer Science (2016) 2016.

[18] K.Y. Lee, D.J. Mooney, Alginate: properties and biomedical applications, Prog. Polym. Sci. 37 (1) (2012) 106–126.

[19] E. Axpe, M.L. Oyen, Applications of alginate-based bioinks in 3D bioprinting, Int. J. Mol. Sci. 17 (12) (2016) 1976.

[20] S. Liu, Y. Hu, J. Zhang, S. Bao, L. Xian, X. Dong, W. Zheng, Y. Li, H. Gao, W. Zhou, Bioactive and biocompatible macroporous scaffolds with tunable performances prepared based on 3D printing of the pre-crosslinked sodium alginate/hydroxyapatite hydrogel ink, Macromol. Mater. Eng. 304 (4) (2019), 1800698.

[21] H. Mishbak, G. Cooper, P. Bartolo, Development and characterization of a photocurable alginate bioink for three-dimensional bioprinting, International Journal of Bioprinting 5 (2) (2019).

[22] B. Joddar, E. Garcia, A. Casas, C.M. Stewart, Development of functionalized multi-walled carbon-nanotube-based alginate hydrogels for enabling biomimetic technologies, Sci. Rep. 6 (1) (2016) 1–12.

[23] T.M. Valentin, A.K. Landauer, L.C. Morales, E.M. DuBois, S. Shukla, M. Liu, L.H. S. Valentin, C. Franck, P.-Y. Chen, I.Y. Wong, Alginate-graphene oxide hydrogels with enhanced ionic tunability and chemomechanical stability for light-directed 3D printing, Carbon 143 (2019) 447–456.

[24] T. Ahlfeld, G. Cidonio, D. Kilian, S. Duin, A. Akkineni, J. Dawson, S. Yang, A. Lode, R. Oreffo, M. Gelinsky, Development of a clay based bioink for 3D cell printing for skeletal application, Biofabrication 9 (3) (2017), 034103.

[25] O. Jeon, Y.B. Lee, H. Jeong, S.J. Lee, D. Wells, E. Alsberg, Individual cell-only bioink and photocurable supporting medium for 3D printing and generation of engineered tissues with complex geometries, Mater. Horiz. 6 (8) (2019) 1625–1631.

[26] J. Park, S.J. Lee, H. Lee, S.A. Park, J.Y. Lee, Three dimensional cell printing with sulfated alginate for improved bone morphogenetic protein-2 delivery and osteogenesis in bone tissue engineering, Carbohydr. Polym. 196 (2018) 217–224.

[27] Z. Lin, M. Wu, H. He, Q. Liang, C. Hu, Z. Zeng, D. Cheng, G. Wang, D. Chen, H. Pan, 3D printing of mechanically stable calcium-free alginate-based scaffolds with tunable surface charge to enable cell adhesion and facile biofunctionalization, Adv. Funct. Mater. 29 (9) (2019), 1808439.

[28] A.C. Daly, G.M. Cunniffe, B.N. Sathy, O. Jeon, E. Alsberg, D.J. Kelly, 3D bioprinting of developmentally inspired templates for whole bone organ engineering, Adv. Healthcare Mater. 5 (18) (2016) 2353–2362.

[29] B. Wang, W. Wang, Y. Yu, Y. Zhang, J. Zhang, Z. Yuan, The study of angiogenesis stimulated by multivalent peptide ligand-modified alginate, Colloids Surf. B Biointerfaces 154 (2017) 383–390.

[30] T. Jiang, J.G. Munguia-Lopez, K. Gu, M.M. Bavoux, S. Flores-Torres, J. Kort-Mascort, J. Grant, S. Vijayakumar, A. De Leon-Rodriguez, A.J. Ehrlicher, Engineering bioprintable alginate/gelatin composite hydrogels with tunable mechanical and cell adhesive properties to modulate tumor spheroid growth kinetics, Biofabrication 12 (1) (2019), 015024.

[31] N. Soltan, L. Ning, F. Mohabatpour, P. Papagerakis, X. Chen, Printability and cell viability in bioprinting alginate dialdehyde-gelatin scaffolds, ACS Biomater. Sci. Eng. 5 (6) (2019) 2976–2987.

[32] T. Jensen, T. Jakobsen, J. Baas, J.V. Nygaard, A. Dolatshahi-Pirouz, M. B. Hovgaard, M. Foss, C. Bünger, F. Besenbacher, K. Søballe, Hydroxyapatite nanoparticles in poly-D, L-lactic acid coatings on porous titanium implants conducts bone formation, J. Biomed. Mater. Res. 95 (3) (2010) 665–672.

[33] J. Kundu, J.H. Shim, J. Jang, S.W. Kim, D.W. Cho, An additive manufacturing-based PCL–alginate–chondrocyte bioprinted scaffold for cartilage tissue engineering, Journal of tissue engineering and regenerative medicine 9 (11) (2015) 1286–1297.

[34] S. Ahadian, R. Rahal, J. Ramón-Azcón, R. Obregón, A. Hasan, Biomaterials in tissue engineering, Tissue engineering for artificial organs: regenerative medicine, smart diagnostics and personalized medicine 1 (2017) 35–83.

[35] M. Aghayan, P. Alizadeh, M. Keshavarz, Multifunctional polyethylene imine hybrids decorated by silica bioactive glass with enhanced mechanical properties, antibacterial, and osteogenesis for bone repair, Mater. Sci. Eng. C 131 (2021), 112534.

[36] R.D. Pedde, B. Mirani, A. Navaei, T. Styan, S. Wong, M. Mehrali, A. Thakur, N. K. Mohtaram, A. Bayati, A. Dolatshahi-Pirouz, Emerging biofabrication strategies for engineering complex tissue constructs, Adv. Mater. 29 (19) (2017), 1606061.

[37] S. Reakasame, A.R. Boccaccini, Oxidized alginate-based hydrogels for tissue engineering applications: a review, Biomacromolecules 19 (1) (2018) 3–21.

[38] F.J. O'brien, Biomaterials & scaffolds for tissue engineering, Mater. Today 14 (3) (2011) 88–95.

[39] S. Zhang, S. Vijayavenkataraman, W.F. Lu, J.Y. Fuh, A review on the use of computational methods to characterize, design, and optimize tissue engineering scaffolds, with a potential in 3D printing fabrication, J. Biomed. Mater. Res. B Appl. Biomater. 107 (5) (2019) 1329–1351.

[40] Z. Wan, P. Zhang, Y. Liu, L. Lv, Y. Zhou, Four-dimensional bioprinting: current developments and applications in bone tissue engineering, Acta Biomater. 101 (2020) 26–42.

[41] R.J. Wade, J.A. Burdick, Engineering ECM signals into biomaterials, Mater. Today 15 (10) (2012) 454–459.

[42] S. Ahadian, A. Khademhosseini, Smart scaffolds in tissue regeneration, Regenerative biomaterials 5 (3) (2018) 125–128.

[43] A. Khademhosseini, R. Langer, A decade of progress in tissue engineering, Nat. Protoc. 11 (10) (2016) 1775–1781.

[44] L. Ghasemi-Mobarakeh, D. Kolahreez, S. Ramakrishna, D. Williams, Key terminology in biomaterials and biocompatibility, Current Opinion in Biomedical Engineering 10 (2019) 45–50.

[45] A. Przekora, The summary of the most important cell-biomaterial interactions that need to be considered during in vitro biocompatibility testing of bone scaffolds for tissue engineering applications, Mater. Sci. Eng. C 97 (2019) 1036–1051.

[46] W. Aljohani, M.W. Ullah, X. Zhang, G. Yang, Bioprinting and its applications in tissue engineering and regenerative medicine, Int. J. Biol. Macromol. 107 (2018) 261–275.

[47] A. Dolcimascolo, G. Calabrese, S. Conoci, R. Parenti, Innovative Biomaterials for Tissue Engineering, Biomaterial-Supported Tissue Reconstruction or Regeneration, IntechOpen2019.

[48] A. Dolatshahi-Pirouz, S. Skeldal, M. Hovgaard, T. Jensen, M. Foss, J. Chevallier, F. Besenbacher, Influence of nanoroughness and detailed surface morphology on structural properties and water-coupling capabilities of surface-bound fibrinogen films, J. Phys. Chem. C 113 (11) (2009) 4406–4412.

[49] D.F. Williams, On the mechanisms of biocompatibility, Biomaterials 29 (20) (2008) 2941–2953.

[50] B.D. Ratner, A.S. Hoffman, F.J. Schoen, J.E. Lemons, W.R. Wagner, S.E. Sakiyama-Elbert, G. Zhang, M.J. Yaszemski, Introduction to Biomaterials Science: an Evolving, Multidisciplinary Endeavor, Academic Press Cambridge, MA, USA2020.

[51] M.A. Heinrich, W. Liu, A. Jimenez, J. Yang, A. Akpek, X. Liu, Q. Pi, X. Mu, N. Hu, R.M. Schiffelers, 3D bioprinting: from benches to translational applications, Small 15 (23) (2019), 1805510.

[52] Y.S. Zhang, K. Yue, J. Aleman, K. Mollazadeh-Moghaddam, S.M. Bakht, J. Yang, W. Jia, V. Dell'Erba, P. Assawes, S.R. Shin, 3D bioprinting for tissue and organ fabrication, Ann. Biomed. Eng. 45 (2017) 148–163.

[53] I. Matai, G. Kaur, A. Seyedsalehi, A. McClinton, C.T. Laurencin, Progress in 3D bioprinting technology for tissue/organ regenerative engineering, Biomaterials 226 (2020), 119536.

[54] S.V. Murphy, A. Atala, 3D bioprinting of tissues and organs, Nat. Biotechnol. 32 (8) (2014) 773–785.

[55] C. Mandrycky, Z. Wang, K. Kim, D.-H. Kim, 3D bioprinting for engineering complex tissues, Biotechnol. Adv. 34 (4) (2016) 422–434.

[56] Y.-C. Li, Y.S. Zhang, A. Akpek, S.R. Shin, A. Khademhosseini, 4D bioprinting: the next-generation technology for biofabrication enabled by stimuli-responsive materials, Biofabrication 9 (1) (2016), 012001.

[57] Q. Yang, B. Gao, F. Xu, Recent advances in 4D bioprinting, Biotechnol. J. 15 (1) (2020), 1900086.

[58] N. Ashammakhi, S. Ahadian, F. Zengjie, K. Suthiwanich, F. Lorestani, G. Orive, S. Ostrovidov, A. Khademhosseini, Advances and future perspectives in 4D bioprinting, Biotechnol. J. 13 (12) (2018), 1800148.

[59] F. Loosli, L. Vitorazi, J.-F. Berret, S. Stoll, Towards a better understanding on agglomeration mechanisms and thermodynamic properties of TiO2 nanoparticles interacting with natural organic matter, Water Res. 80 (2015) 139–148.

[60] L. Maldonado, J. Kokini, An optimal window for the fabrication of Edible Polyelectrolyte Complex Nanotubes (EPCNs) from bovine serum albumin (BSA) and sodium alginate, Food Hydrocolloids 77 (2018) 336–346.

[61] M.M. Perera, N. Ayres, Dynamic covalent bonds in self-healing, shape memory, and controllable stiffness hydrogels, Polym. Chem. 11 (8) (2020) 1410–1423.

[62] J.W. Boley, W.M. Van Rees, C. Lissandrello, M.N. Horenstein, R.L. Truby, A. Kotikian, J.A. Lewis, L. Mahadevan, Shape-shifting structured lattices via multimaterial 4D printing, Proc. Natl. Acad. Sci. USA 116 (42) (2019) 20856–20862.

[63] A. Sydney Gladman, E.A. Matsumoto, R.G. Nuzzo, L. Mahadevan, J.A. Lewis, Biomimetic 4D printing, Nat. Mater. 15 (4) (2016) 413–418.

[64] A. Garate, A. Murua, G. Orive, R.M. Hernández, J.L. Pedraz, Stem cells in alginate bioscaffolds, Ther. Deliv. 3 (6) (2012) 761–774.

[65] Q. Liu, Q. Li, S. Xu, Q. Zheng, X. Cao, Preparation and properties of 3D printed alginate–chitosan polyion complex hydrogels for tissue engineering, Polymers 10 (6) (2018) 664.

[66] J.M. Unagolla, A.C. Jayasuriya, Hydrogel-based 3D bioprinting: a comprehensive review on cell-laden hydrogels, bioink formulations, and future perspectives, Appl. Mater. Today 18 (2020), 100479.

[67] R.F. Quadrado, A.R. Fajardo, Fast decolorization of azo methyl orange via heterogeneous Fenton and Fenton-like reactions using alginate-Fe2+/Fe3+ films as catalysts, Carbohydrate Polymers 177 (2017) 443–450.

[68] I. Braccini, S. Pérez, Molecular basis of Ca2+-induced gelation in alginates and pectins: the egg-box model revisited, Biomacromolecules 2 (4) (2001) 1089–1096.

[69] S. Kumbar, C. Laurencin, M. Deng, Natural and Synthetic Biomedical Polymers, Newnes2014.

[70] C.K. Kuo, P.X. Ma, Ionically crosslinked alginate hydrogels as scaffolds for tissue engineering: Part 1. Structure, gelation rate and mechanical properties, Biomaterials 22 (6) (2001) 511–521.

[71] A.C. Hernández-González, L. Téllez-Jurado, L.M. Rodríguez-Lorenzo, Alginate hydrogels for bone tissue engineering, from injectables to bioprinting: a review, Carbohydr. Polym. 229 (2020), 115514.

[72] S. Datta, R. Barua, J. Das, Importance of Alginate Bioink for 3D Bioprinting in Tissue Engineering and Regenerative Medicine, Alginates—Recent Uses of This Natural Polymer, 2020.

[73] X. Han, A. Alu, H. Liu, Y. Shi, X. Wei, L. Cai, Y. Wei, Biomaterial-assisted biotherapy: a brief review of biomaterials used in drug delivery, vaccine development, gene therapy, and stem cell therapy, Bioact. Mater. 17 (2022) 29–48.

[74] R.B. Elliott, L. Escobar, P.L. Tan, M. Muzina, S. Zwain, C. Buchanan, Live encapsulated porcine islets from a type 1 diabetic patient 9.5 yr after xenotransplantation, Xenotransplantation 14 (2) (2007) 157–161.

[75] S. Duin, S. Bhandarkar, S. Lehmann, E. Kemter, E. Wolf, M. Gelinsky, B. Ludwig, A. Lode, Viability and functionality of neonatal porcine islet-like cell clusters bioprinted in alginate-based bioinks, Biomedicines 10 (6) (2022) 1420.

[76] E. Ruvinov, S. Cohen, Alginate biomaterial for the treatment of myocardial infarction: progress, translational strategies, and clinical outlook: from ocean algae to patient bedside, Adv. Drug Deliv. Rev. 96 (2016) 54–76.

[77] M.Ø. Dalheim, J. Vanacker, M.A. Najmi, F.L. Aachmann, B.L. Strand, B. E. Christensen, Efficient functionalization of alginate biomaterials, Biomaterials 80 (2016) 146–156.

[78] G. Choe, S. Oh, J.M. Seok, S.A. Park, J.Y. Lee, Graphene oxide/alginate composites as novel bioinks for three-dimensional mesenchymal stem cell printing and bone regeneration applications, Nanoscale 11 (48) (2019) 23275–23285.

[79] F. Olate-Moya, L. Arens, M. Wilhelm, M.A. Mateos-Timoneda, E. Engel, H. Palza, Chondroinductive alginate-based hydrogels having graphene oxide for 3D printed scaffold fabrication, ACS applied materials & interfaces 12 (4) (2020) 4343–4357.

[80] M. Monavari, S. Homaeigohar, M. Fuentes-Chandia, Q. Nawaz, M. Monavari, A. Venkatraman, A.R. Boccaccini, 3D printing of alginate dialdehyde-gelatin (ADA-GEL) hydrogels incorporating phytotherapeutic icariin loaded mesoporous SiO2-CaO nanoparticles for bone tissue engineering, Mater. Sci. Eng. C 131 (2021), 112470.

[81] A.N. Leberfinger, S. Dinda, Y. Wu, S.V. Koduru, V. Ozbolat, D.J. Ravnic, I. T. Ozbolat, Bioprinting functional tissues, Acta Biomater. 95 (2019) 32–49.

[82] S. Uman, A. Dhand, J.A. Burdick, Recent advances in shear-thinning and self-healing hydrogels for biomedical applications, J. Appl. Polym. Sci. 137 (25) (2020), 48668.

[83] D. Chimene, R. Kaunas, A.K. Gaharwar, Hydrogel bioink reinforcement for additive manufacturing: a focused review of emerging strategies, Advanced materials 32 (1) (2020), 1902026.

[84] G. Cidonio, M. Glinka, Y.-H. Kim, J.M. Kanczler, S.A. Lanham, T. Ahlfeld, A. Lode, J.I. Dawson, M. Gelinsky, R.O. Oreffo, Nanoclay-based 3D printed scaffolds promote vascular ingrowth ex vivo and generate bone mineral tissue in vitro and in vivo, Biofabrication 12 (3) (2020), 035010.

[85] L. Li, S. Qin, J. Peng, A. Chen, Y. Nie, T. Liu, K. Song, Engineering gelatin-based alginate/carbon nanotubes blend bioink for direct 3D printing of vessel constructs, Int. J. Biol. Macromol. 145 (2020) 262–271.

[86] H. Li, S. Liu, L. Lin, Rheological study on 3D printability of alginate hydrogel and effect of graphene oxide, International Journal of Bioprinting 2 (2) (2016).

[87] J. Li, X. Liu, J.M. Crook, G.G. Wallace, 3D printing of cytocompatible graphene/alginate scaffolds for mimetic tissue constructs, Front. Bioeng. Biotechnol. 8 (2020) 824.

[88] L. Suo, H. Wu, P. Wang, Z. Xue, J. Gao, J. Shen, The improvement of periodontal tissue regeneration using a 3D-printed carbon nanotube/chitosan/sodium alginate composite scaffold, J. Biomed. Mater. Res. B Appl. Biomater. 111 (1) (2023) 73–84.

[89] M. Lafuente-Merchan, S. Ruiz-Alonso, F. García-Villén, A. Zabala, A.M.O. de Retana, I. Gallego, L. Saenz-del-Burgo, J.L. Pedraz, 3D bioprinted hydroxyapatite or graphene oxide containing nanocellulose-based scaffolds for bone regeneration, Macromol. Biosci. 22 (11) (2022), 2200236.

[90] J. Adhikari, M.S. Perwez, A. Das, P. Saha, Development of hydroxyapatite reinforced alginate–chitosan based printable biomaterial-ink, Nano-Structures & Nano-Objects 25 (2021), 100630.

[91] J.L. Dávila, M.A. d'Ávila, Rheological evaluation of Laponite/alginate inks for 3D extrusion-based printing, Int. J. Adv. Des. Manuf. Technol. 101 (1) (2019) 675–686.

[92] Y. Jin, C. Liu, W. Chai, A. Compaan, Y. Huang, Self-supporting nanoclay as internal scaffold material for direct printing of soft hydrogel composite structures in air, ACS applied materials & interfaces 9 (20) (2017) 17456–17465.

[93] C. Sharma, A.K. Dinda, P.D. Potdar, C.-F. Chou, N.C. Mishra, Fabrication and characterization of novel nano-biocomposite scaffold of chitosan–gelatin–alginate–hydroxyapatite for bone tissue engineering, Mater. Sci. Eng. C 64 (2016) 416–427.

[94] S.T. Bendtsen, S.P. Quinnell, M. Wei, Development of a novel alginate-polyvinyl alcohol-hydroxyapatite hydrogel for 3D bioprinting bone tissue engineered scaffolds, J. Biomed. Mater. Res. 105 (5) (2017) 1457–1468.

[95] T.T. Demirtaş, G. Irmak, M. Gümüşderelioğlu, A bioprintable form of chitosan hydrogel for bone tissue engineering, Biofabrication 9 (3) (2017), 035003.

[96] D. Chawla, T. Kaur, A. Joshi, N. Singh, 3D bioprinted alginate-gelatin based scaffolds for soft tissue engineering, Int. J. Biol. Macromol. 144 (2020) 560–567.

[97] N. Huettner, T.R. Dargaville, A. Forget, Discovering cell-adhesion peptides in tissue engineering: beyond RGD, Trends Biotechnol. 36 (4) (2018) 372–383.

[98] T. Boontheekul, H.-J. Kong, D.J. Mooney, Controlling alginate gel degradation utilizing partial oxidation and bimodal molecular weight distribution, Biomaterials 26 (15) (2005) 2455–2465.

[99] N.G. Genes, J.A. Rowley, D.J. Mooney, L.J. Bonassar, Effect of substrate mechanics on chondrocyte adhesion to modified alginate surfaces, Arch. Biochem. Biophys. 422 (2) (2004) 161–167.

[100] N. Huebsch, P.R. Arany, A.S. Mao, D. Shvartsman, O.A. Ali, S.A. Bencherif, J. Rivera-Feliciano, D.J. Mooney, Harnessing traction-mediated manipulation of the cell/matrix interface to control stem-cell fate, Nat. Mater. 9 (6) (2010) 518–526.

[101] A.G. Solano, J. Dupuy, H. Therriault, B. Liberelle, N. Faucheux, M.-A. Lauzon, N. Virgilio, B. Paquette, An alginate-based macroporous hydrogel matrix to trap cancer cells, Carbohydrate Polymers 266 (2021), 118115.

[102] X. Tan, E. Jain, M.N. Barcellona, E. Morris, S. Neal, M.C. Gupta, J.M. Buchowski, M. Kelly, L.A. Setton, N. Huebsch, Integrin and syndecan binding peptide-conjugated alginate hydrogel for modulation of nucleus pulposus cell phenotype, Biomaterials 277 (2021), 121113.

[103] L. Cheng, B. Yao, T. Hu, X. Cui, X. Shu, S. Tang, R. Wang, Y. Wang, Y. Liu, W. Song, Properties of an alginate-gelatin-based bioink and its potential impact on cell migration, proliferation, and differentiation, Int. J. Biol. Macromol. 135 (2019) 1107–1113.

[104] C. Ma, J.-B. Choi, Y.-S. Jang, S.-Y. Kim, T.-S. Bae, Y.-K. Kim, J.-M. Park, M.-H. Lee, Mammalian and fish gelatin methacryloyl–alginate interpenetrating polymer network hydrogels for tissue engineering, ACS Omega 6 (27) (2021) 17433–17441.

[105] J. Sun, H. Tan, Alginate-based biomaterials for regenerative medicine applications, Materials 6 (4) (2013) 1285–1309.

[106] J. Jia, D.J. Richards, S. Pollard, Y. Tan, J. Rodriguez, R.P. Visconti, T.C. Trusk, M. J. Yost, H. Yao, R.R. Markwald, Engineering alginate as bioink for bioprinting, Acta Biomater. 10 (10) (2014) 4323–4331.

[107] A.A. Aldana, F.L. Morgan, S. Houben, L.M. Pitet, L. Moroni, M.B. Baker, Biomimetic double network hydrogels: combining dynamic and static crosslinks to enable biofabrication and control cell-matrix interactions, J. Polym. Sci. 59 (22) (2021) 2832–2843.

[108] T. Kreller, T. Distler, S. Heid, S. Gerth, R. Detsch, A. Boccaccini, Physico-chemical modification of gelatine for the improvement of 3D printability of oxidized alginate-gelatine hydrogels towards cartilage tissue engineering, Mater. Des. 208 (2021), 109877.

[109] O. Jeon, D.S. Alt, S.M. Ahmed, E. Alsberg, The effect of oxidation on the degradation of photocrosslinkable alginate hydrogels, Biomaterials 33 (13) (2012) 3503–3514.

[110] O. Jeon, R. Marks, D. Wolfson, E. Alsberg, Dual-crosslinked hydrogel microwell system for formation and culture of multicellular human adipose tissue-derived stem cell spheroids, J. Mater. Chem. B 4 (20) (2016) 3526–3533.

[111] O. Jeon, J.E. Samorezov, E. Alsberg, Single and dual crosslinked oxidized methacrylated alginate/PEG hydrogels for bioadhesive applications, Acta Biomater. 10 (1) (2014) 47–55.

[112] O. Jeon, Y.B. Lee, S.J. Lee, N. Guliyeva, J. Lee, E. Alsberg, Stem cell-laden hydrogel bioink for generation of high resolution and fidelity engineered tissues with complex geometries, Bioact. Mater. 15 (2022) 185–193.

[113] D. Heyes, A. Brańka, Interactions between microgel particles, Soft Matter 5 (14) (2009) 2681–2685.

[114] B.R. Saunders, B. Vincent, Microgel particles as model colloids: theory, properties and applications, Adv. Colloid Interface Sci. 80 (1) (1999) 1–25.
[115] B. Kessel, M. Lee, A. Bonato, Y. Tinguely, E. Tosoratti, M. Zenobi-Wong, 3D bioprinting of macroporous materials based on entangled hydrogel microstrands, Adv. Sci. 7 (18) (2020) 2001419.
[116] A. Ding, O. Jeon, R. Tang, Y.B. Lee, S.J. Lee, E. Alsberg, Cell-laden multiple-step and reversible 4D hydrogel actuators to mimic dynamic tissue morphogenesis, Adv. Sci. 8 (9) (2021), 2004616.
[117] A. Ding, O. Jeon, D. Cleveland, K.L. Gasvoda, D. Wells, S.J. Lee, E. Alsberg, Jammed micro-flake hydrogel for four-dimensional living cell bioprinting, Adv. Mater. 34 (15) (2022), 2109394.
[118] A. Ding, S.J. Lee, R. Tang, K.L. Gasvoda, F. He, E. Alsberg, 4D cell-condensate bioprinting, Small 18 (36) (2022), 2202196.
[119] O. Jeon, Y.B. Lee, T.J. Hinton, A.W. Feinberg, E. Alsberg, Cryopreserved cell-laden alginate microgel bioink for 3D bioprinting of living tissues, Mater. Today Chem. 12 (2019) 61–70.
[120] L.T. Somasekharan, N. Kasoju, R. Raju, A. Bhatt, Formulation and characterization of alginate dialdehyde, gelatin, and platelet-rich plasma-based bioink for bioprinting applications, Bioengineering 7 (3) (2020) 108.
[121] H. Shehzad, L. Zhou, Y. Wang, J. Ouyang, G. Huang, Z. Liu, Z. Li, Effective biosorption of U (VI) from aqueous solution using calcium alginate hydrogel beads grafted with amino-carbamate moieties, J. Radioanal. Nucl. Chem. 321 (2) (2019) 605–615.
[122] S. Maiz-Fernández, L. Pérez-Álvarez, L. Ruiz-Rubio, J.L. Vilas-Vilela, S. Lanceros-Mendez, Polysaccharide-based in situ self-healing hydrogels for tissue engineering applications, Polymers 12 (10) (2020) 2261.
[123] J. Ye, S. Fu, S. Zhou, M. Li, K. Li, W. Sun, Y. Zhai, Advances in hydrogels based on dynamic covalent bonding and prospects for its biomedical application, Eur. Polym. J. 139 (2020), 110024.
[124] R. Tan, Z. She, M. Wang, Z. Fang, Y. Liu, Q. Feng, Thermo-sensitive alginate-based injectable hydrogel for tissue engineering, Carbohydrate Polymers 87 (2) (2012) 1515–1521.
[125] Y. Chen, R. Zhang, B. Zheng, C. Cai, Z. Chen, H. Li, H. Liu, A biocompatible, stimuli-responsive, and injectable hydrogel with triple dynamic bonds, Molecules 25 (13) (2020) 3050.
[126] L. Wang, W. Zhou, Q. Wang, C. Xu, Q. Tang, H. Yang, An injectable, dual responsive, and self-healing hydrogel based on oxidized sodium alginate and hydrazide-modified poly (ethyleneglycol), Molecules 23 (3) (2018) 546.
[127] S. Lanzalaco, E. Armelin, Poly (N-isopropylacrylamide) and copolymers: a review on recent progresses in biomedical applications, Gels 3 (4) (2017) 36.
[128] A. Kirillova, R. Maxson, G. Stoychev, C.T. Gomillion, L. Ionov, 4D biofabrication using shape-morphing hydrogels, Adv. Mater. 29 (46) (2017), 1703443.
[129] G. Constante, I. Apsite, H. Alkhamis, M. Dulle, M. Schwarzer, A. Caspari, A. Synytska, S. Salehi, L. Ionov, 4D biofabrication using a combination of 3D printing and melt-electrowriting of shape-morphing polymers, ACS Appl. Mater. Interfaces 13 (11) (2021) 12767–12776.
[130] J. Lai, X. Ye, J. Liu, C. Wang, J. Li, X. Wang, M. Ma, M. Wang, 4D printing of highly printable and shape morphing hydrogels composed of alginate and methylcellulose, Mater. Des. 205 (2021), 109699.
[131] M. Champeau, D.A. Heinze, T.N. Viana, E.R. de Souza, A.C. Chinellato, S. Titotto, 4D printing of hydrogels: a review, Adv. Funct. Mater. 30 (31) (2020), 1910606.
[132] S.E. Bakarich, R. Gorkin III, M.I.H. Panhuis, G.M. Spinks, 4D printing with mechanically robust, thermally actuating hydrogels, Macromol. Rapid Commun. 36 (12) (2015) 1211–1217.
[133] H. Ko, M.C. Ratri, K. Kim, Y. Jung, G. Tae, K. Shin, Formulation of sugar/hydrogel inks for rapid thermal response 4D architectures with sugar-derived macropores, Sci. Rep. 10 (1) (2020) 7527.
[134] C. Sun, H. Jia, K. Lei, D. Zhu, Y. Gao, Z. Zheng, X. Wang, Self-healing hydrogels with stimuli responsiveness based on acylhydrazone bonds, Polymer 160 (2019) 246–253.
[135] C.N. Cheaburu, O.N. Ciocoiu, G. Staikos, C. Vasile, Thermoresponsive sodium alginate-g-poly (N-isopropylacrylamide) copolymers III. Solution properties, J. Appl. Polym. Sci. 127 (5) (2013) 3340–3348.
[136] M.H. Kim, J.-C. Kim, H.Y. Lee, J. Dai Kim, J.H. Yang, Release property of temperature-sensitive alginate beads containing poly (N-isopropylacrylamide), Colloids and surfaces B: Biointerfaces 46 (1) (2005) 57–61.
[137] J. Zhang, Z. Cui, R. Field, M.G. Moloney, S. Rimmer, H. Ye, Thermo-responsive microcarriers based on poly (N-isopropylacrylamide), Eur. Polym. J. 67 (2015) 346–364.
[138] Y.B. Lee, O. Jeon, S.J. Lee, A. Ding, D. Wells, E. Alsberg, Induction of four-dimensional spatiotemporal geometric transformations in high cell density tissues via shape-changing hydrogels, Adv. Funct. Mater. 31 (24) (2021), 2010104.
[139] T.T. Vu, M. Gulfam, S.-H. Jo, S.-H. Park, K.T. Lim, Injectable and biocompatible alginate-derived porous hydrogels cross-linked by IEDDA click chemistry for reduction-responsive drug release application, Carbohydrate Polymers 278 (2022), 118964.
[140] D.M. Roquero, E. Katz, "Smart" alginate hydrogels in biosensing, bioactuation and biocomputing: state-of-the-art and perspectives, Sensors and Actuators Reports 4 (2022), 100095.
[141] P. Cao, L. Tao, J. Gong, T. Wang, Q. Wang, J. Ju, Y. Zhang, 4D printing of a sodium alginate hydrogel with step-wise shape deformation based on variation of crosslinking density, ACS Appl. Polym. Mater. 3 (12) (2021) 6167–6175.
[142] C. Cui, D.-O. Kim, M.Y. Pack, B. Han, L. Han, Y. Sun, L.-H. Han, 4D printing of self-folding and cell-encapsulating 3D microstructures as scaffolds for tissue-engineering applications, Biofabrication 12 (4) (2020), 045018.